USAMRICD-TR-17-07

A Preliminary Study of Chronic Lung Toxicity in Rats Following a Single Inhalation Challenge to Sulfur Mustard: Assessment of the Effect of Mesenchymal Stem Cell Treatment

Alfred M. Sciuto
Jennifer L. Collins
Timothy R. Varney
Jannitt B. Simons
Ashley M. Rodriguez
Dorian S. Olivera

November 2017

US Army Medical Research Institute of Chemical Defense
2900 Ricketts Point Road
Aberdeen Proving Ground, MD 21010-5400

an element of the

US Army Medical Research and Materiel Command

DISPOSITION INSTRUCTIONS:

Destroy this report when no longer needed. Do not return to the originator.

DISCLAIMERS:

The views expressed in this technical report are those of the author(s) and do not reflect the official policy of the Department of Army, Department of Defense, or the U.S. Government.

The experimental protocol was approved by the Animal Care and Use Committee at the United States Army Medical Research Institute of Chemical Defense, and all procedures were conducted in accordance with the principles stated in the Guide for the Care and Use of Laboratory Animals and the Animal Welfare Act of 1966 (P.L. 89-544), as amended.

The use of trade names does not constitute an official endorsement or approval of the use of such commercial hardware or software. This document may not be cited for purposes of advertisement.

REPORT DOCUMENTATION PAGE

Form Approved
OMB No. 0704-0188

1. REPORT DATE *(DD-MM-YYYY)*	**2. REPORT TYPE**	**3. DATES COVERED** *(From - To)*
November 2017	Technical Report	November 2008 – June 2013

4. TITLE AND SUBTITLE
A Preliminary Study of Chronic Lung Toxicity in Rats Following a Single Inhalation Challenge to Sulfur Mustard: Assessment of the Effect of Mesenchymal Stem Cell Treatment

5a. CONTRACT NUMBER

5b. GRANT NUMBER
3.F0009 07 RC C & CBM.RESP. 01.10.009RC

5c. PROGRAM ELEMENT NUMBER

6. AUTHOR(S)
Sciuto, AM, Collins, JL, Varney, TR., Simons, JB., Rodriguez, A, Olivera DS

5d. PROJECT NUMBER

5e. TASK NUMBER

5f. WORK UNIT NUMBER

7. PERFORMING ORGANIZATION NAME(S) AND ADDRESS(ES)

US Army Medical Research Institute of Chemical Defense
ATTN: MCMR-CDR-ET
2900 Ricketts Point Road
Aberdeen Proving Ground, MD 21010-5400

8. PERFORMING ORGANIZATION REPORT NUMBER

USAMRICD-TR-17-07

9. SPONSORING / MONITORING AGENCY NAME(S) AND ADDRESS(ES)

Defense Threat Reduction Agency
8725 John J. Kingman Road STOP 6201
Fort Belvoir, VA 22060-6201

10. SPONSOR/MONITOR'S ACRONYM(S)
DTRA

11. SPONSOR/MONITOR'S REPORT NUMBER(S)

12. DISTRIBUTION / AVAILABILITY STATEMENT

Approved for public release; distribution unlimited.

13. SUPPLEMENTARY NOTES

14. ABSTRACT
Sulfur mustard (SM) is a blistering agent (vesicant) that causes severe chemical burns to the skin, eyes, and airways. Used as a chemical warfare agent in past conflicts, many surviving casualties continue to suffer from permanent lung injuries. Mechanisms and timing of these pathologies remain unknown. Modelling the mouth-breathing human, rats were anesthetized, intubated, ventilated and then exposed for 10 min to either vehicle or nebulized SM. Rats were euthanized at various time points ≤ 6 months post-exposure. Over time, blood gas chemistries, antioxidant response elements, inflammatory markers and histopathology revealed that SM inhalation resulted clinical decrements consistent with the progression of severe lung injury observed in humans. Alveolar exudates, edema, mediator responses and inflammation peaked early in the acute phase of injury and correlated with chronic obstructive pulmonary disease (COPD) that can be described as a progressive asthmatic-like condition. Based on this information, we evaluated the effects of a 6-hour post-exposure mesenchymal stem cell therapeutic approach and found it effective in reducing SM-induced edema, necrosis, inflammation, and death at 3-6 weeks. This study provided the first long-term examination of SM-induced lung injury and demonstrates the feasibility of stem cell therapy for SM inhalation injury.

15. SUBJECT TERMS
Rats, sulfur mustard, aerosol, lung, toxicology, physiology, chronic effects, stem cell therapy, inflammatory mediators, pulmonary function, histopathology, redox cycle, chemical warfare agent, medical chemical defense

16. SECURITY CLASSIFICATION OF:			**17. LIMITATION OF ABSTRACT**	**18. NUMBER OF PAGES**	**19a. NAME OF RESPONSIBLE PERSON**
a. REPORT	**b. ABSTRACT**	**c. THIS PAGE**			Alfred M. Sciuto
UNCLASSIFIED	UNCLASSIFIED	UNCLASSIFIED	UNLIMITED	60	**19b. TELEPHONE NUMBER** *(include area code)* 410-436-5115

ACKNOWLEDGMENT: This study was supported by the Defense Threat Reduction Agency of the Department of Defense Agency project 3.F0009 07 RC C & CBM.RESP. 01.10.009RC. We would also like to thank Drs. Larry Mitcheltree and Tony Alves for their expertise in reading pathology and Ms. Tracey Hamilton for her superb technical advice. In addition, we would wish to express our gratitude for the expert technical assistance of Ms. Elizabeth Lyman and Ms. Alicia Witriol on this project.

ABSTRACT

Sulfur mustard (SM) is a blistering agent (vesicant) that causes severe chemical burns to the skin, eyes, and airways. SM was used as a chemical warfare agent (CWA) in the Iran/Iraq conflict, and more than half of surviving SM-exposed casualties continue to suffer from permanent lung injuries. SM remains a serious threat with no effective antidote. Despite over 90 years of study since SM was developed as a CWA, the mechanisms and timing of the development of these pathologies remain poorly defined. To model the mouth-breathing human, rats were intubated and ventilated for 10 min with nebulized SM or vehicle to achieve total doses of 0, 0.5, 1.75, 2.25, and 3 mg/kg (335-402 mg/m^3). Pulmonary function was analyzed by whole-body plethysmography. Rats were euthanized at various time points ≤ 6 months post-exposure, blood chemistry was analyzed, and lungs were subjected to pathologic analysis. Mid-study data showed elevated pCO_2 and lowered blood pH and pO_2, which correlated with upper airway necrosis and measurements of pulmonary function in the 24-48 hrs after 3 mg/kg SM exposure. For the 6-month animals, the period between 3 and 7 weeks presented a significant challenge because approximately 60-70% of the high exposure dose group (3 mg/kg) and 40-50% of the 2.25 mg/kg group either died or required withdrawal from the study during this timeframe. Over time, blood gas chemistries, antioxidant response elements, inflammatory markers and histopathology revealed that SM inhalation resulted in a range of physiological and toxicological decrements consistent with the progression of severe lung injury observed in humans. In addition, alveolar exudates, edema, and inflammation peaked early in the acute phase of injury and correlated with compensatory changes in pulmonary function and/or respiratory distress. Based on histopathology, pulmonary respiratory function, and mediator responses, chronic obstructive pulmonary disease (COPD) is evident and can be described as an asthmatic-like condition that progresses over time. Data indicate that 3-7 weeks post-exposure may be a crucial window in the progression of SM inhalation injury, and that therapeutic intervention prior to and concurrent with this time point may offer the best approach. Based on this information, we evaluated the effects of a 6-hour post-exposure mesenchymal stem cell therapeutic approach and found it effective in reducing SM-induced edema, necrosis, inflammation, and death at 3-6 weeks. This study provides the first long-term examination of SM-induced lung injury and systemic effects, and further demonstrates the feasibility of stem cell therapy for SM inhalation injury.

INTRODUCTION

Sulfur mustard (SM) is a vesicant. SM ($C_4H_8Cl_2S$) is also known as Yellow Cross, Lost, S-Lost, H or Yperite. It was first used as a chemical warfare agent (CWA) in 1917 and more recently during the Iraq-Iran conflict in the 1980's. SM vapor was responsible for about 80% of the chemical exposure deaths during World War I (Hurst and Smith, 2008). Exposure to SM caused numerous injuries, acute as well as chronic, and ultimately death (Kehe and Szinicz, 2005). SM is easily synthesized from common industrial chemicals. Although an oily liquid with a moderately low vapor pressure, SM can be aerosolized or heated to produce vapor and as such can travel long distances during windy conditions. As a vapor, it is 5.4 times as dense as air, hugs the ground, and can be persistent in the environment from days to several weeks. It can remain a threat for some time in various aqueous environments and has caused skin blisters when handled many years after submergence (Aasted *et al*., 1985; Wulf *et al.*, 1985). SM is an alkylating agent and reactive molecular cross-linker (Wheeler 1962). Chemical reactions involving SM can stimulate and produce free radicals (Korkmaz *et al.* 2006; Brimfield *et al.*, 2012), resulting in oxidative stress, which can escalate via an inflammatory chain-reaction (Laskin *et al.*, 2010; Balali-Mood and Hefazi, 2005). The reactive chemical nature of SM is due to the cyclization formation of an episulfonium ion which can combine with numerous nucleophilic sites. SM has been shown to be toxic in both *in vitro* (Meier *et al*., 1996; Sawyer, 1999; Atkins *et al*., 2000; Ray *et al*., 2008; Pohl *et al*., 2009) and *in vivo* experimental models (Vijayaraghavan *et al*., 1991; Gold and Scharf, 1995; Anderson *et al*., 1996; Casillas *et al.*, 1997; Rao *et al*., 1999; van Helden *et al*., 2004; Dillman *et al*., 2005; Sciuto *et al*. 2000, 2007; Fairhall *et al*., 2010).

SM can be readily absorbed into tissues with much of it finding its way into the circulation, thereby causing systemic effects. The principal targets of SM toxicity are ocular, dermal, and lung tissue surfaces. Bone marrow, a site of cell proliferation, is also a target of SM toxicity (Dacre and Goldman, 1996). While exposure through ocular and dermal routes is incapacitating, most fatalities are a result of inhalation (Eisenmenger *et al*., 1991). Symptoms of exposure are delayed, with a latency of ~24 hrs for inhalation exposures. SM forms fluid-filled blisters, and associated pain may take several hours. Following dermal exposure, pain is immediate with tissue damage and clinical effects occurring hours to days later. Higher exposures have lower latency times to symptoms (acute). Inhaled SM is largely absorbed in the upper airway and rarely penetrates to the lung parenchyma unless the concentration or duration of exposure or both are sufficiently high. In humans, following wartime inhalation exposure to SM, reports have identified bronchopneumonia, chest tightness, and in long-term survivors, chronic bronchitis, lung fibrosis, productive cough, and chronic obstructive pulmonary disease (Ghanei and Harandi, 2007). Injury can develop slowly, becoming much more intense over time. More detailed clinical manifestations can be found in Willems (1989).

While there is not a direct causative link between SM exposure and cancer from battlefield exposures, workers occupationally exposed to mustard during production had a higher incidence of respiratory, skin and blood cancer (Nishimura *et al*., 2016; Pechura and Rall, 1993). Gopinath and Mowat (2014) provide a pathological description of the presence of cancer in rat lung tissue. Experimentally, Kan *et al.* (2008) provided some evidence of a possible causal link between the inhalation of SM and cancer in rats exposed to a single high dose of SM for 10 min. The current study was designed to satisfy an information gap by using an animal exposure model to investigate the effects of a single inhalation challenge to SM over a 6-month time period. While there have been studies that terminate at 7 (Malaviya *et al.*, 2010) or 30 days (Mishra *et al.*,

2012), they do not match the equivalent timeline vs toxicity when compared to the human temporal exposure-response effects seen in humans (Ghanei and Harandi, 2007). These data provided evidence that longer-termed health consequences after a single exposure episode to SM are manifested in responses years after battlefield exposure to SM. Acute effects following exposure to SM include initial pain, discomfort, increased nasal secretions, sneezing, coughing, sore throat within 4-16 hrs; late onset of laryngeal lesions; tracheal and large bronchial inflammation/necrosis; sloughing of airway tissue lining; and hemoptysis. These effects are largely dose-dependent. Chronic consequences include bronchiectasis, COPD, emphysema, fibrosis, asthma, bronchiolitis obliterans, hemorrhagic inflammation, tracheobronchial stenosis, pneumonia, septicemia, ulcers and strictures, gas exchange disorders, and damaged lung surfactant. Although studies on treatments have had limited success recently in several animal models, they are generally focused on more acute exposure-effect responses (Kumar *et al*., 2001; Jugg *et al*., 2013;Veress *et al.*, 2015).

The complex character of inhaled SM toxicity creates a challenge to field effective medical countermeasures since a mixture of toxidromes are manifested over time. In this regard, we tested the feasibility of mesenchymal stem cell (MSC) treatment against inhaled SM. MSC treatment has been shown to be effective in mice challenged with endotoxin (Gupta *et al.*, 2007), bleomycin (Ortiz *et al.*, 2003) and phosgene (Zhang *et al.*, 2016). Preliminary data cited herein may provide a possible therapeutic role for treating SM-induced lung injury.

MATERIALS AND METHODS

Animals. Adult Male Sprague-Dawley (SD) rats (Charles River Laboratories, Wilmington, MA) weighing 240-300 g on the exposure day were used. Animals were housed individually after exposure under standard conditions with a 12 hours light/dark cycle and food and water were available *ad libitum*. The study protocol was approved by the Institute Animal Care and Use Committee, USAMRICD, Aberdeen Proving Ground, MD. Research at USAMRICD was conducted in compliance with the *Animal Welfare Act* as amended (2007) and other federal statutes and regulations relating to animals and experiments involving animals and adheres to principles stated in the *Guide for the Care and Use of Laboratory Animals*, National Research Council, published by the National Academy Press, 1996.

Challenge Agent and Dose. All exposures occurred over a 10-minute period with concentrations ranging from 0, 0.5, 1.75, 2.25, and 3 mg/kg (335-402 mg/m^3). The entire exposure system was confined within an inhalation exposure chamber (glovebox). Exposure concentrations were based on earlier published findings that 350 µg of vaporized SM over 50 min will produce lung injury in spontaneously breathing rats (Anderson *et al.*, 1996).

Study Design. Male SD rats were anesthetized with 90 mg/kg ketamine and 10 mg/kg xylazine intramuscularly. Rats were placed in supine position, and a modified and polished smooth-bore glass pasture pipette (~5 cm. in length) was inserted into the trachea using a modified laryngoscope and PE90 tubing as a stylus guide. The glass insert was held in place with mildly adhesive tape, and the rat was then transferred to the exposure chamber. A single 10-minute exposure to SM was delivered using a closed-to-atmosphere inhalation system via mechanical ventilation **(Figure 1).** The respiration rate was determined by the baseline rates for each animal. SM was delivered by a small animal ventilator (Harvard Model 683, Harvard Apparatus, Holliston, MA) and set for a tidal volume of 2.5-3 mL and a respiratory rate of 60-

90 breaths/ minute. Because conscious rats can control their respiration when subjected to an irritant environment, anesthetized and ventilated procedures were used to standardize the minute volume (respiration rate x tidal volume) for each exposed rat. SM was delivered from a closed circuit standard nebulizer system (Aeroneb, Aerogen Inc., Marietta, GA). The Aeroneb unit has a volume of 10 mL and can deliver approximately 0.22 mL/min at a mean particle size of 1.6 µm, well within the range for deep lung deposition. The nebulizer was placed in series between the ventilator and the glass endotracheal insert; thus, SM aerosol was administered by the action of mechanical ventilation to produce an aerosolized exposure stream. This allowed for an even and consistent delivery of SM to the peripheral airway by bypassing the nasal passages, a site of detoxification, and also served to assist the rat for ventilation in the event that agent irritation affected the breathing pattern. Because of solubility issues aerosolizing neat agent, SM was diluted in a 75% ETOH + 25% saline solution (ethanol/saline controls) for ease and consistency of delivery. During the course of exposure, a sample from the aerosol stream was taken for MINCAMS (Mini Chemical Agent Monitor) quantitative analysis. Exhaled gases from the rat were routed via a unidirectional Rudolph valve (Hans-Rudolf Inc., Shawnee, KS) into a flask neutralized with 50 ml of 5% bleach, then through an activated charcoal canister, and finally exited the system through the exhaust HEPA filter. Following SM exposure and after a 10-minute room air off-gas time period, rats were extubated, and placed in recovery posture.

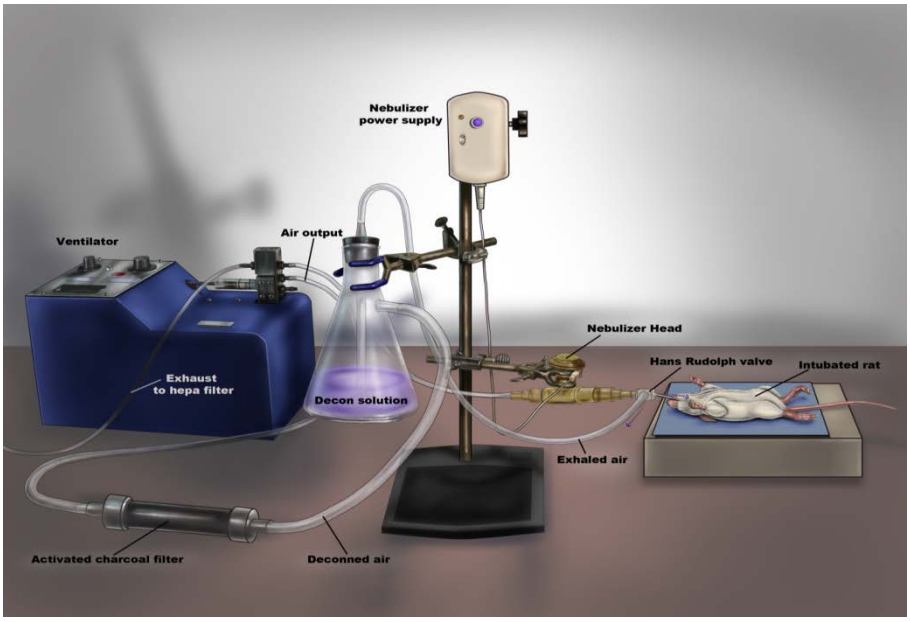

Figure 1. Anesthetized intratracheal SM aerosol exposure and decontamination system.

Pulmonary Dynamics Assessment. Across all time points and SM doses reported herein, respiratory dynamics were assessed. Prior to exposure, all conscious rats were placed in the whole-body plethysmograph (WBP) for approximately 2 hrs to establish baselines for the following respiratory function parameters: tidal volume (TV- mL), respiratory frequency (R_f - breaths/min), minute volume (MV- mL/min), inspired and expired time rates (T_i; T_e - sec), putative bronchoconstriction (Enhanced Pause, EPAU), and peak expiratory and inspiratory flow

rates (PEF; PIF- mL/sec) (Buxco Inc. Sharon, CT). After this baseline phase, rats were removed, anesthetized as stated above, and exposed to the SM aerosol for 10 minutes. Immediately following exposure, each anesthetized rat was returned to the WBP for an additional 6 hrs of respiratory dynamics assessment. Within the first 90-120 min in the WBP, all rats recovered from anesthesia. Following this 6-hour assessment recovered rats were placed in their respective cages and returned to the animal room facility overnight. Over the following days and months survivors were returned to the WBP for a 2-hour respiratory function assessment daily at the same time for the first 72 hrs and then weekly for the next 6 months for all of the time points.

Perfusion, Necropsy and Histopathology. At predetermined designated or culled time points after SM-exposure, rats were deeply anesthetized as described, and a ventral midline incision was made to expose the thoracic cavity. Rats were perfused with 500 mL of 0.89% normal saline (4.5 grams sodium chloride in 500 mL distilled water) and 250 mL of 10% neutral buffered formalin (Sigma) at a perfusion rate of 40-60 mL/min using a Cole Parmer Masterflex perfusion pump (Model 77200-60**).** Perfusate was injected into the right heart ventricle to perfuse the lungs. Immediately following perfusion, the lungs were harvested and placed into 10% neutral buffered formalin at biosafety level 2 (BSL-2) for 24-72 hrs at 4ºC. To properly fix the lungs, fixative was slowly instilled into the trachea using a blunted 18 gauge needle until the lungs were inflated**.** Immediately following perfusion, lungs were harvested and post-fixed in 10% formalin for 18-24 hrs at 4ºC. The trachea was then ligated with suture to prevent leakage. Lung sections comprising the right cranial, right middle, right caudal, and accessory lung lobe, left lung lobe, and trachea were scored by veterinary pathologists blinded to the study groups. Following fixation, lung tissues were processed in paraffin and serially sectioned at 5-10 microns. Lung sections were stained with H&E (hematoxylin and eosin) for evaluating the extent of pathology, Movat pentachrome or Gomeri trichrome for studying the magnitude of pulmonary fibrosis or periodic acid Schiff for examining the degree of mucus production. H&E stained lung sections were qualitatively scored from 0 to 4 with 0=none; 1=trace; 2=mild (1-10%); 3=moderate (10-50%); 4=severe (>50%) for acute pathological changes and evaluated for proliferative changes. The extent of pulmonary fibrosis and mucus production in the lungs was quantified using an imaging analysis program (ImagePro Plus; Media Cybernetics, Inc., Silver Spring, MD).

***Bronchoalveolar Lavage Fluid (BALF) Analysis*.** Following euthanasia, a tracheotomy was performed, and a cannula inserted and tied to prevent leakage. Up to 5 mL of sterile saline was infused into the lungs and gently washed back and forth 3-5 times. The final bronchoalveolar lavage fluid (BALF) volume was recorded, and the recovered sample split for analysis of cytokines/chemokines, glutathione redox state, LDH, protein, etc. BALF aliquots were stored at -80°C. BALF was assayed using a microplate spectrophotometer (SPECTRAMax Plus 384, Molecular Devices, Sunnyvale, CA) for biomarkers such as glutathione peroxidase (GPx, Cayman, Ann Arbor, MI), glutathione (GSH, Oxis Research, Portland, OR), and catalase (CAT, Cayman). Myeloperoxidase (MPO), a marker of leukocyte infiltration, and macrophage inhibitory protein (MIP-1α), a measure of macrophage damage, were also determined (Cayman, Ann Arbor. MI). Protein content was determined using the Lowry method (Lowry *et al*., 1951).

***Blood SM Adduct Analysis*.** At selected time points, arterial blood plasma concentrations of systemic SM-plasma protein adducts were obtained following exsanguination. SM adducts were analyzed using a gas chromatographic/mass spectrophotometric technique as described by Capacio *et al.* (2008).

Cytokine analysis. Cytokine levels were determined in BALF with a Bio-Rad Bio-Plex suspension array system (Hercules, CA). Standard immunoassay kits were used to measure cytokines IL-1α, IL-1β, IL-2, IL-4, IL-5, IL-6, IL-7, IL-12(p70), IL-13, IL-17, IL-18, GRO-KC, TNFα, M-CSF, RANTES, MIP-1α, MIP-3α, and EPO (BioRad, Hercules, CA).

***Blood gas analysis*.** Animals were anesthetized and euthanized by exsanguination by blood draw from the aorta. Blood gases were measured using the i-STAT Handheld System (Abbott Laboratories , Abbott Park, IL). Parameters analyzed included pCO_2, pH, pO_2, hematocrit (Hct %), total hemoglobin (THb g/dl), and O_2 saturation. Blood was immediately analyzed using an IRMA TruePoint Blood Analysis System (ITC, Edison, NJ).

Mesenchymal Stem Cell (MSC) Treatment. For MSC studies, cells were derived from a green fluorescent protein expressing transgenic rat line and were isolated from the femoral bone marrow of Lewis rats, cultured in fibronectin-coated flasks, and frozen in treatment aliquots for subsequent application. On the day of exposure, cells were reconstituted in physiologic saline to $2x10^6$ cells/mL, and viability > 70% was confirmed. Rats exposed to either 2.25 mg/kg SM or ethanol/saline were used to evaluate MSC therapy. Approximately 4-6 hrs post-exposure (PE), rats received either MSC suspension ($2x10^6$ cells + saline flush = total volume 2 mL) or an equivalent volume of saline only, administered via jugular catheter. Following MSC therapy, animals were euthanized as mentioned above at 5 weeks PE based on several observations: animal weights dramatically declined, animal losses increased, pulmonary dynamics were altered, and pathologic abnormalities increased.

Data Analysis. Initially, this study was intended to investigate temporal dose-response effects of inhaled SM; the results herein will largely involve comparisons of trending data due to insufficient samples at selected time points and concentrations. All data are expressed as the mean ± standard error. Parametric data analyses were performed on lung wet/dry weight ratios, body weights, pulmonary dynamics, glutathione, blood gas parameters, etc., using two- (time and dose) or one-factor (dose) ANOVAs. If data were significant post hoc tests such as the Tukey's or Dunnett's C multiple comparison method were performed (Dunnett's C test was used when group variances were unequal). A Chi-square and/or Kruskal Wallis test was used on categorical data to compare dose groups. Significance level was set at $p \leq 0.05$. Where appropriate, marginal data are shown.

RESULTS

Figure 2 shows that body weight loss changed radically over time in the highest SM exposure groups. Higher SM exposures resulted in signs of stress, including pulmonary crackles, piloerection, porphyrin staining, and lack of weight gain, which were phenomena not observed in ethanol/saline controls. Statistical analyses demonstrated a significant deviation (blunted weight gain) in the 3.0 mg/kg group at the 3-week PE point. This was mirrored in the 1.75 mg/kg group, but not in the 2.25 mg/kg group. By 8 weeks PE, the animals which deviated from controls died, and the weight time course thereafter blends in with the other exposure groups' weight-loss time courses. It is apparent that the reduced weight gain at 3 weeks PE is a predictor of later death, as those animals that survived to their scheduled cull dates did not deviate from the ethanol/saline controls, while those that died or were culled early due to a decline in health or respiratory distress did show the diminished weight gain compared to ethanol/saline controls.

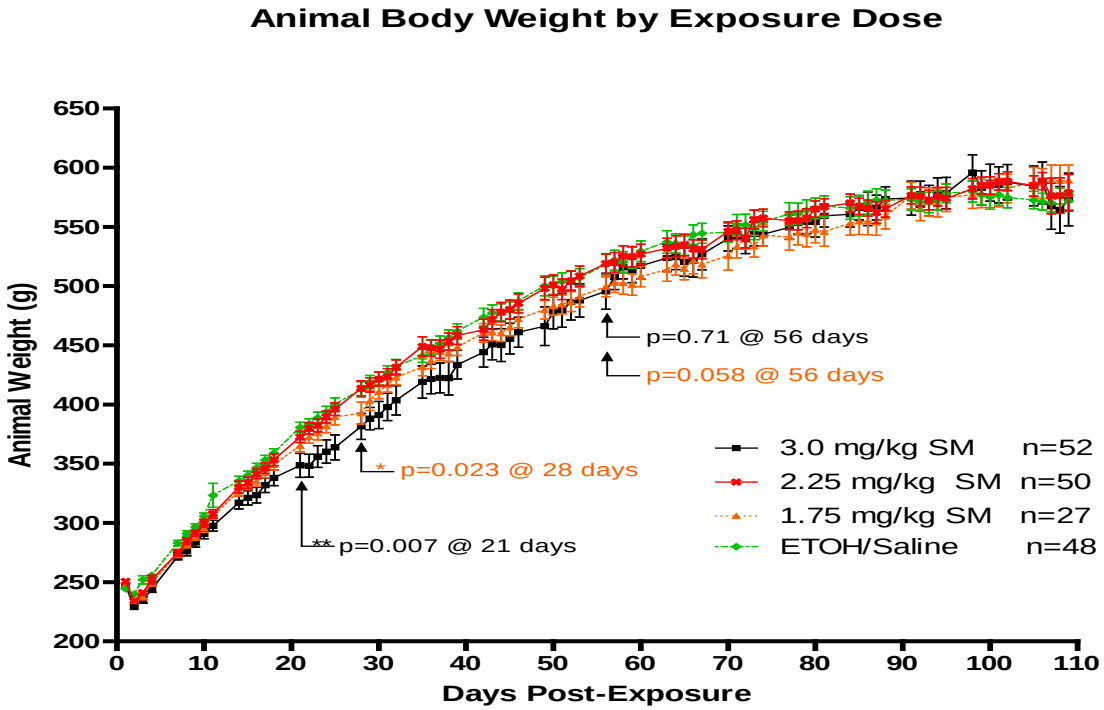

Figure 2. Temporal SM dose-response changes in rat body weight and group sample sizes. Two-way ANOVA results are expressed as mean ± SEM.

Figure 3 shows the Kaplan-Meier survival curve representing the timing of animal loss by dose.

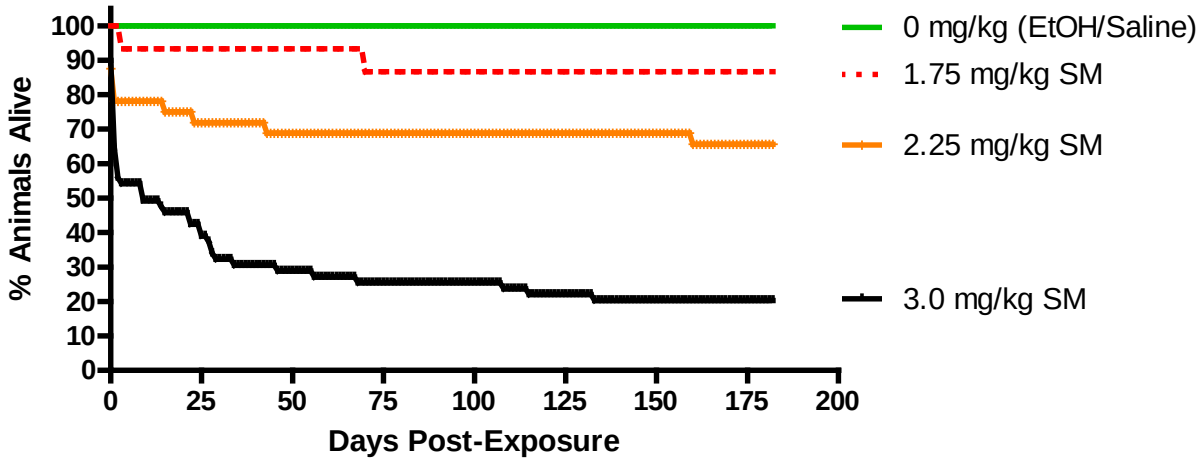

Figure 3. Kaplan-Meier survival dose-response curves for SM aerosolized over time.

Table 1 shows the actual survival rates from 1-180 days PE. At 6 months the 1.75 mg/kg exposure resulted in an LCt_{13}, the 2.25 mg/kg exposure produced an LCt_{35}, and the 3.0 mg/kg exposure group showed an LCt_{80}. Approximately 30% of the 3.0 mg/kg-exposed animals died within 24 hrs PE **(Table 1).** A second wave of fatalities followed at the three-week PE time point, when an additional 15% of 3.0 mg/kg animals were lost. This correlates tightly in time with the blunted weight gain shown in **Figure 2**. The same delayed losses occurred in the 2.25 mg/kg group within approximately the same time frame, while delayed losses were also seen in the 1.75 mg/kg exposure group. Acute losses overall were dose-dependent becoming greater with increasing SM dosing. Delayed losses were greater and earlier with increasing SM exposure dose. At lower SM exposure there were fewer losses from the acute injury, with delayed injury occurring later and being milder in character. Interestingly, these data clearly indicate that a single 10-minute exposure to aerosolized SM resulted in a two-phase injury: an acute phase when approximately 40% of all exposure-related death occurred within the first two days, and a latent phase injury when the remaining 30% perished within 3-5 weeks as symptoms of pulmonary distress and severe inflammation became more apparent.

TABLE 1. Temporal SM dose-response survival rates (%) following a single 10–minute inhalation challenge to SM**.**

Days	E/SC (n=19)	1.75 mg/kg (n=22)	2.25 mg/kg (n=44)	3.0 mg/kg (n=72)
-1	100	100	100	100
0	100	100	84.1	90.2
Post-Exposure				
1	100	100	61.3	70.8
2	100	95.4	61.3	61.1
3	100	95.4	61.3	56.9
9	100	95.4	61.3	51.3
11	100	95.4	61.3	50
14	100	95.4	61.3	48.6
15	100	95.4	59.1	45.8
17	100	95.4	59.1	44.4
22	100	95.4	59.1	41.6
23	100	95.4	56.8	41.6
25	100	95.4	56.8	38.8
28	100	95.4	56.8	34.7
29	100	90.9	56.8	33.3
34	100	90.9	56.8	31.9
37	100	90.9	56.8	30.5
43	100	90.9	54.5	30.5
46	100	90.9	54.5	29.1
49	100	90.9	54.5	26.3
56	100	90.9	54.5	25
68	100	90.9	54.5	23.6
70	100	86.3	54.5	23.6
77	100	81.8	54.5	23.6
108	100	81.8	54.5	22.2
115	100	81.8	54.5	20.8
128	100	81.8	54.5	19.4
133	100	81.8	54.5	18.1
161	100	81.8	52.2	18.1
180	100	81.8	52.2	18.1

Blood Gases

Figures 4A-D show the temporal dose-dependent changes in arterial blood gas data. Temporal arterial blood O_2 saturation for the 3 mg/kg-exposed group at 24 hrs PE was approximately 39% lower than for time-matched ethanol/saline controls, 57% vs 93%, respectively. At 25 days PE this difference decreased to 24% lower than ethanol/saline controls. At 180 days PE most groups were nearly equivalent except for the 2.25 mg/kg group, which was 20% lower than ethanol/saline controls, indicating compromised lung gas exchange **(Figure 4A).**

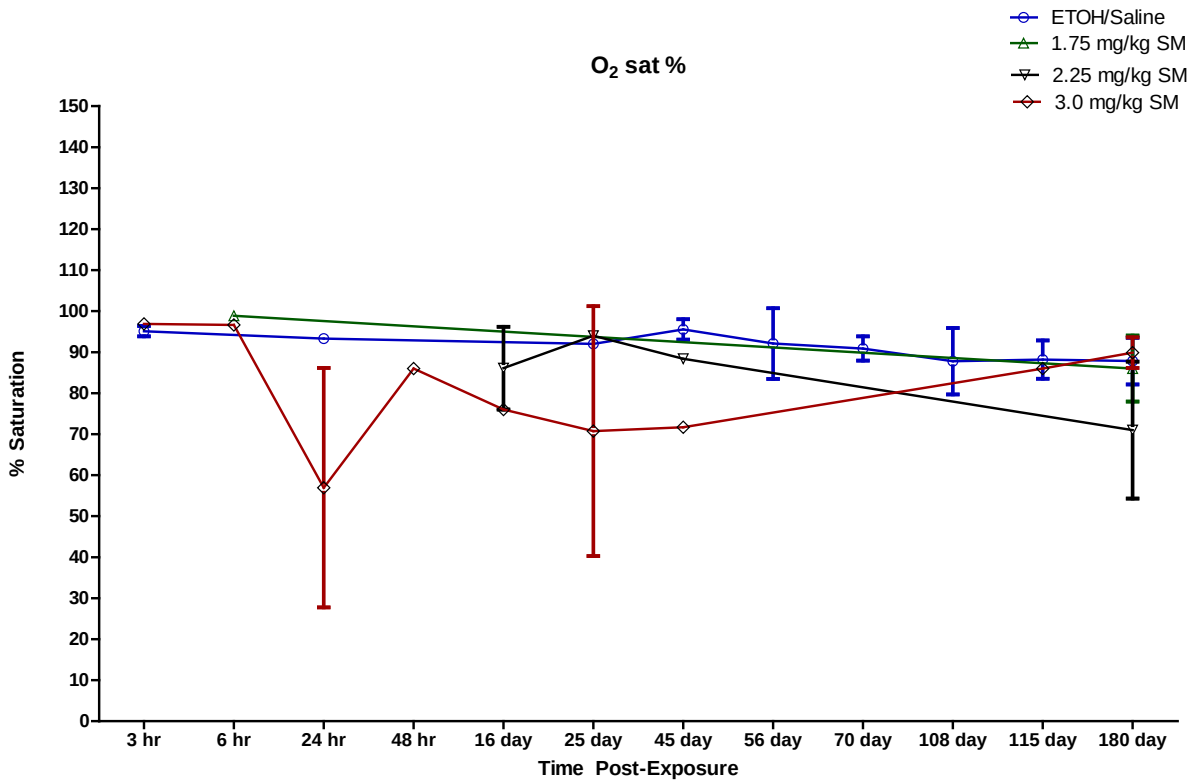

Figure 4A. Temporal dose-response SM-induced changes in arterial blood O_2 saturation.

Figure 4B shows that pO_2 begins to decline about 6 hrs PE in the 3.0 mg/kg SM-exposed rats after starting in the 92-95 mmHg range. At 24 hrs PE there was a 42% decrement in pO_2 between 3.0 mg/kg SM-exposed rats and time-matched ethanol/saline controls. The pO_2 in the 3.0 mg/kg-exposed group remained around 42 mm/Hg as far out as 45days and reached only about 60 mmHg in survivors at 180 days PE. Conditions of hypoxemia were evident in the 3.0 mg/kg dose group up to about 10 weeks PE. The pO_2 in the 1.75 mg/kg-exposed group steadily declined from 79 to 59 mmHg, a decrease of about 26%, from 3 hrs to 180 days PE, whereas at 25 days 2.25 mg/kg SM-exposed rats showed a 31% decrement in pO_2 from 79 to 51 mmHg between 25 and 180 days PE.

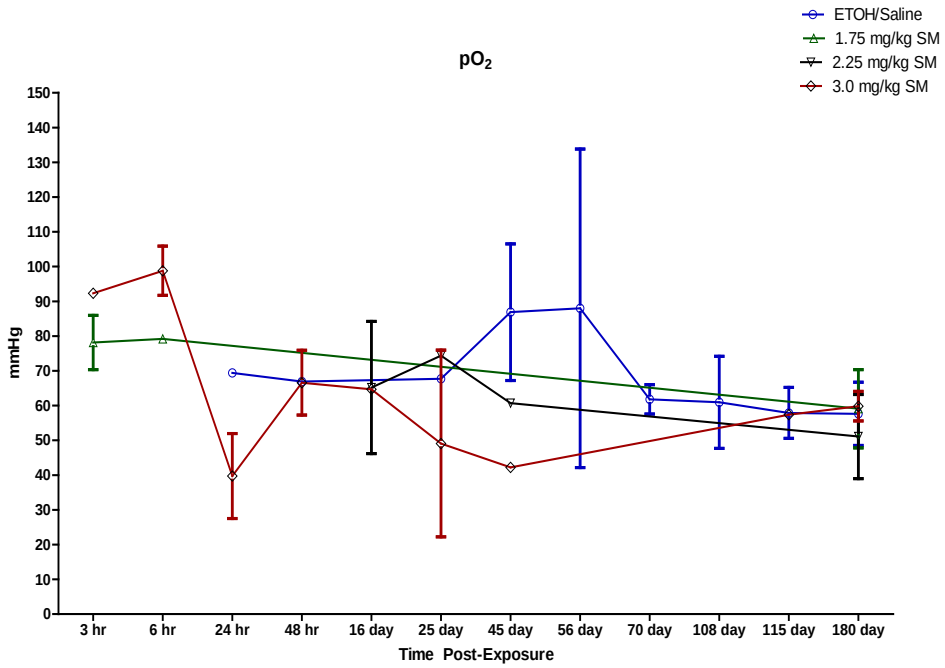

Figure 4B. Temporal dose-response SM-induced changes in arterial blood pO_2.

Mean arterial pCO_2 in both the 1.75 and 3.0 mg/kg SM-exposed groups was within normal limits 3-6 hrs PE **(Figure 4C).** However, at 24 hrs the 3.0 mg/kg-exposed group increased to 87 mmHg, a 100% increase from 3 hrs PE. After 45 days there was a downward trend to 49 mmHg, which was slightly lower than in ethanol/saline controls. There was yet another upsurge in pCO_2 at 108 days PE for the 3.0 mg/kg group to 91 mmHg, 85% higher than time-matched ethanol/saline controls, suggesting a renewed decrement in the rats' capacity to expel excess CO_2. For the 2.25 mg/kg–exposed rats there was a steady decline in respiratory function as shown by a trending increase in pCO_2 from 61 to 91 mmHg between day16 and 180 days, indicating compromised lung function and a chronic exposure-response state.

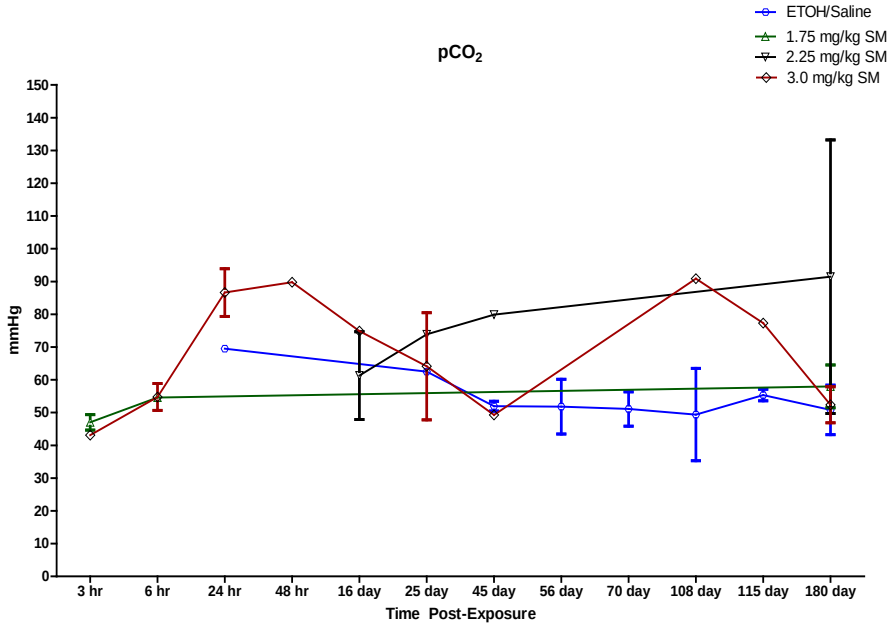

Figure 4C. Temporal dose-response SM-induced changes in arterial blood pCO_2.

Mean arterial pH in both the 1.75 and 3.0 mg/kg SM-exposed rats was within normal physiological limits, approximately 7.39, 3 hrs PE **(Figure 4D).** At 24 hrs PE pH in the 3.0 mg/kg-exposed group decreased to 7.17 versus 7.37 for time-matched ethanol/saline controls. Mean arterial pH in the 2.25 mg/kg group steadily declined from 7.35 to 7.19 between 16-180 days PE, whereas in ethanol/saline controls it was well-maintained during the entire PE period. The decrements in pH, pO_2, and increases in pCO_2, especially in the early phases of the study, clearly indicated a condition of respiratory acidosis.

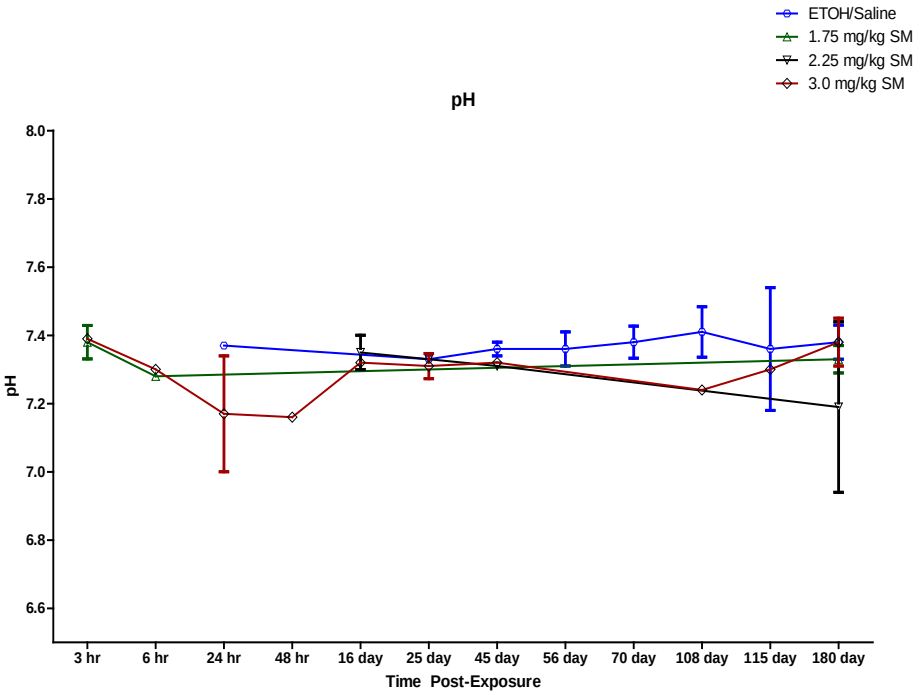

Figure 4D Temporal dose-response SM-induced changes in arterial blood pH**.**

As an adjunct to blood gas chemistries, total hemoglobin (THb) and hematocrit (Hct) were analyzed. Although the temporal results for both THb and Hct fall within the published normal range for Sprague-Dawley rats used in this study (Otto *et al.*, 2015), we did observe changes between the highest SM inhalation concentration and ethanol/saline controls at 4 weeks PE. There was a 27% increase in THb to 16.3 g/dl for 3.0 mg/kg SM group versus 12.8 g/dl for ethanol/saline controls. Similarly, Hct increased 28% for 3.0 mg/kg SM animals, to 48% versus 37.4% for the ethanol/saline group at the same time point. Both THb and Hct were near normal values for the remainder of the study (**data not shown**). These conditions equate to polycythemia and likely indicated an increase in hemoglobin production, either to compensate for poor cardiopulmonary function or possibly due to SM-induced bone marrow dysregulation.

Blood SM Adducts

To determine the presence of adducts following a 10-minute inhalation challenge to aerosolized SM, whole arterial blood samples were collected over time. Data reflect individual rats euthanized at each time point up to 24 hrs PE. These were then analyzed for the presence of

adducts following a single 10-minute exposure to aerosolized SM. **Figure 5** shows the initial dose-response relationship over the first 24 hrs PE. The doses tested in this study, 1.75, 2.25, and 3.0 mg/kg, resulted in the presence of adducts which ranged from 150-325 nM, signifying the validation of the exposure model for establishing markers of SM exposure following an inhalation challenge. SM adducts appear to reach a maximum for the 2.25-3.0 mg/kg-exposed groups of about 400-600 nM within 3 hrs PE. While there was a dose-response relationship among all doses tested over time, it appears that at the two highest doses this was not the case. This could be related to saturation processes in the lung responsible for the delivery of SM to the blood and/or animal to animal variability. **Figure 6** provides a 140-day profile in individual rats of SM adducts in the blood for the exposure concentrations tested. There is a clear presence of SM protein adducts for 1.75-3.0 mg/kg up to 7 days PE with minimal amounts observed up to 21 days PE. The levels of detection and quantification in this model were 12.5 nM and 5.0 nM, respectively.

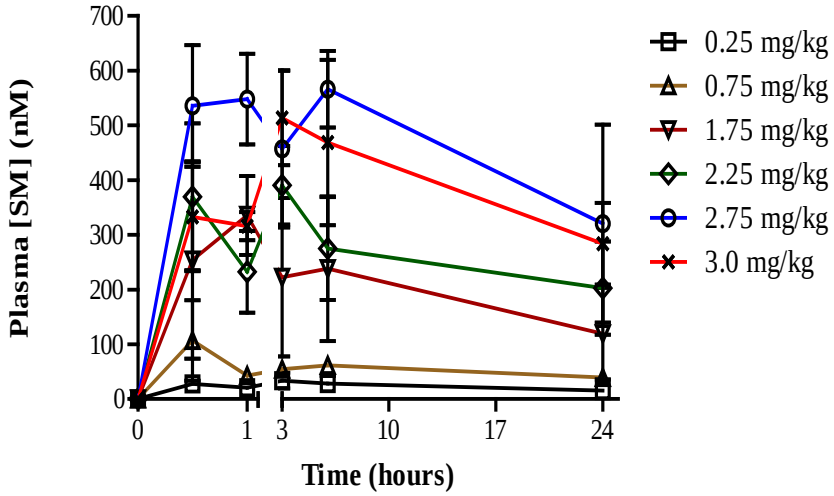

Figure 5. Twenty-four-hour dose-response effects of inhaled aerosolized SM on blood plasma adduct formation.

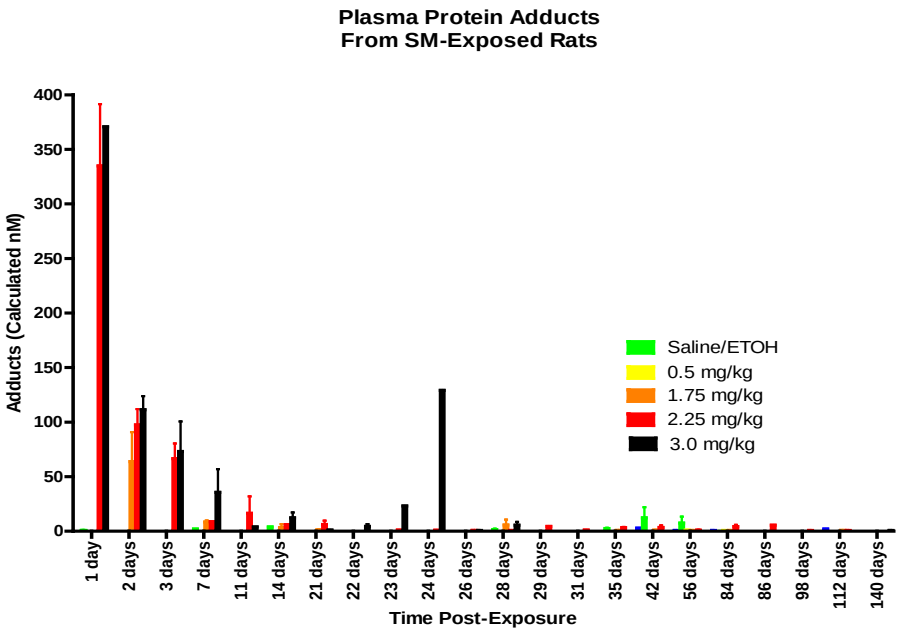

Figure 6. Long-termed effects of inhaled aerosolized SM on the presence of blood plasma adduct formation.

Respiratory Dynamics

WBP analyses was performed on all animals exposed to a single 10-minute challenge of aerosolized SM. WBP data for PEF, Te, MV and EPAU were collected for the first six hrs PE and then over two-hour intervals for the first 72 hrs **(Figures 7A-10A).** Thereafter, data were collected weekly across a two-hour time period between 1-11 weeks **(Figures 7B-10B)** and 12-26 weeks PE **(Figures 7C-10C).** All two-hour measurements occurred from 10 AM-12 PM to match the original WBP collection. During the first 3-4 hrs PE, responses were in part the result of recovery from anesthesia.

T_e values over the initial 72-hour PE time frame largely indicated that all dosed animals exhibited decreased expiration time ranging from 35-50% slower than time-matched ethanol/saline controls especially in the 3- to 6-hour time interval **(Figure 7A).** At 24 hrs T_e trended toward ethanol/saline controls. Between 3-7 weeks PE, the 3.0 mg/kg group showed substantially lower expiration times compared with time-matched controls, averaging about 20% faster than time-matched ethanol/saline controls **(Figure 7B).** Faster expiration times remained from weeks 12-26 for the highest SM-exposed group. Additionally, at week 13, both the 1.75 and 2.25 mg/kg groups also showed lower expiration times, compared to time-matched ethanol/saline controls. The reduction in expiration times was greatest around 23-24 weeks PE before returning to near controls levels at the end of the study **(Figure 7C).**

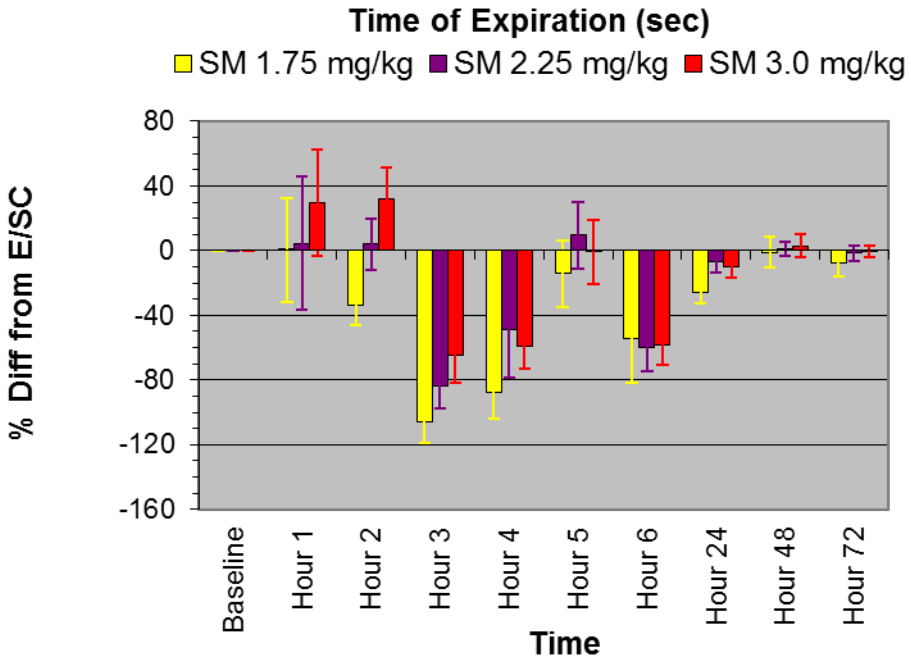

Figure 7A. A 1- to 72-hour profile of the effects of inhaled aerosolized SM on time of expiration. Data shown as percent difference from ethanol/saline controls.

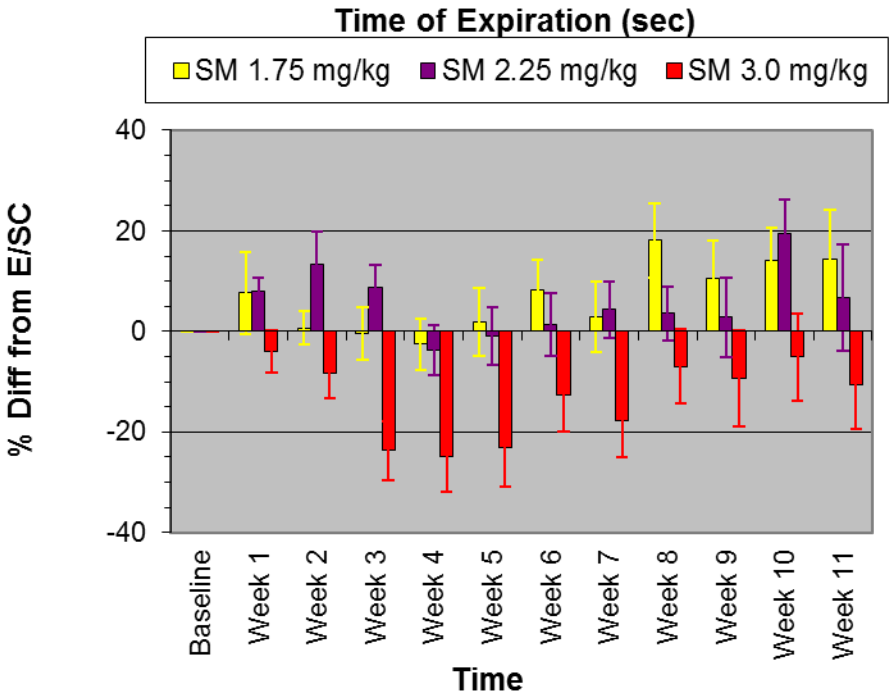

Figure 7B. A 1- to 11-week profile of the effects of inhaled aerosolized SM on time of expiration. Data shown as percent difference from ethanol/saline controls.

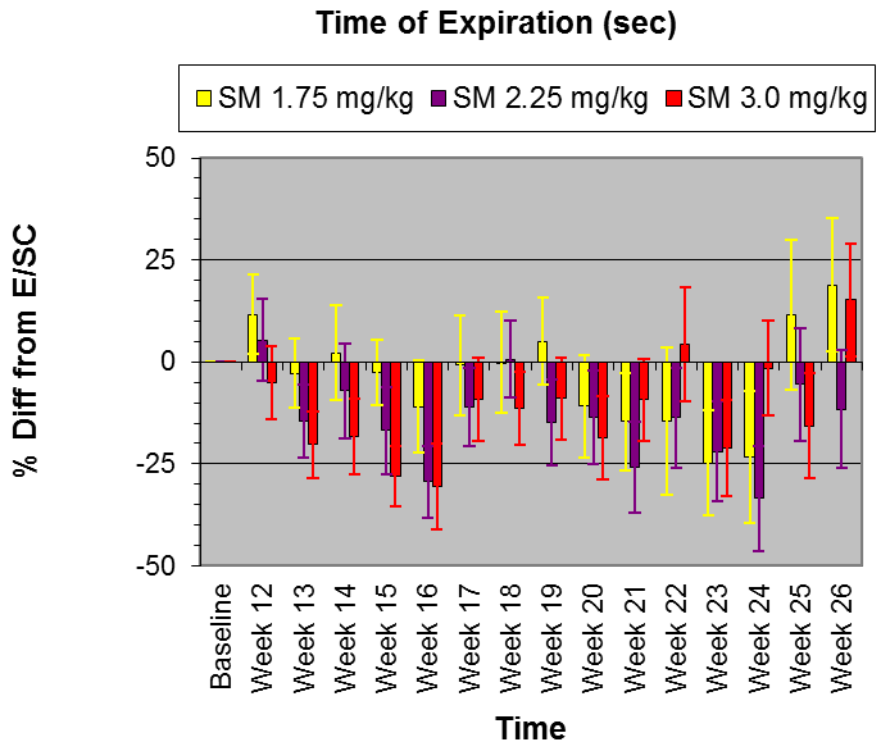

Figure 7C. A 12- to 26-week profile of the effects of inhaled aerosolized SM on time of expiration. Data shown as percent difference from ethanol/saline controls

Figure 8A shows the temporal effects of SM inhalation on PEF over the first 72 hrs PE. There was a 45-80% increase in expired air flow in the 3.0 mg/kg group 24 hrs PE compared with time-matched ethanol/saline controls. Increased PEF was persistent in the high-dose SM-exposed rats over the 11-week time frame reaching a rate nearly 200% faster than ethanol/saline controls at week 4 **(Figure 8B)** and approximately 240% at week 15 **(Figure 8C).** At week 20 PE, PEF rates began to approach ethanol/saline controls levels for all SM-exposed groups. However, while doses of 1.75 to 2.25 mg/kg SM showed no marked increases vs ethanol/saline controls early on, there was about a 50% increase in PEF for 1.75 mg/kg between weeks 22-24, indicating a latency of modified airflow months after the initial challenge **(Figure 7C).** This may be a compensatory mechanism whereby the animals are attempting to increase airflow rates by respiring faster because of the increased presence of SM-induced pseudomembranous casts in the airways.

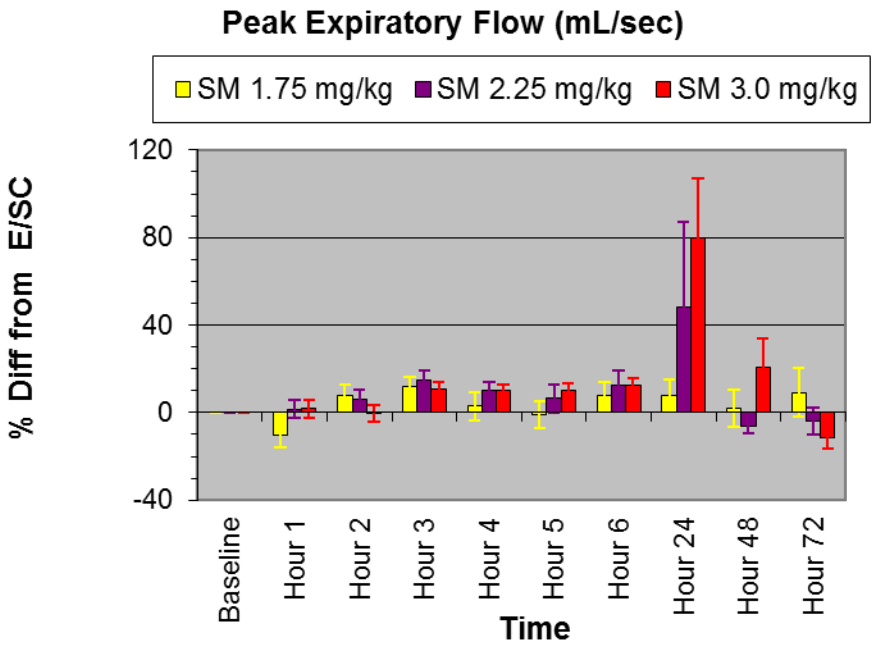

Figure 8A. A 1- to 72-hour profile of the effects of inhaled aerosolized SM on peak expiratory flow. Data shown as percent difference from ethanol/saline controls.

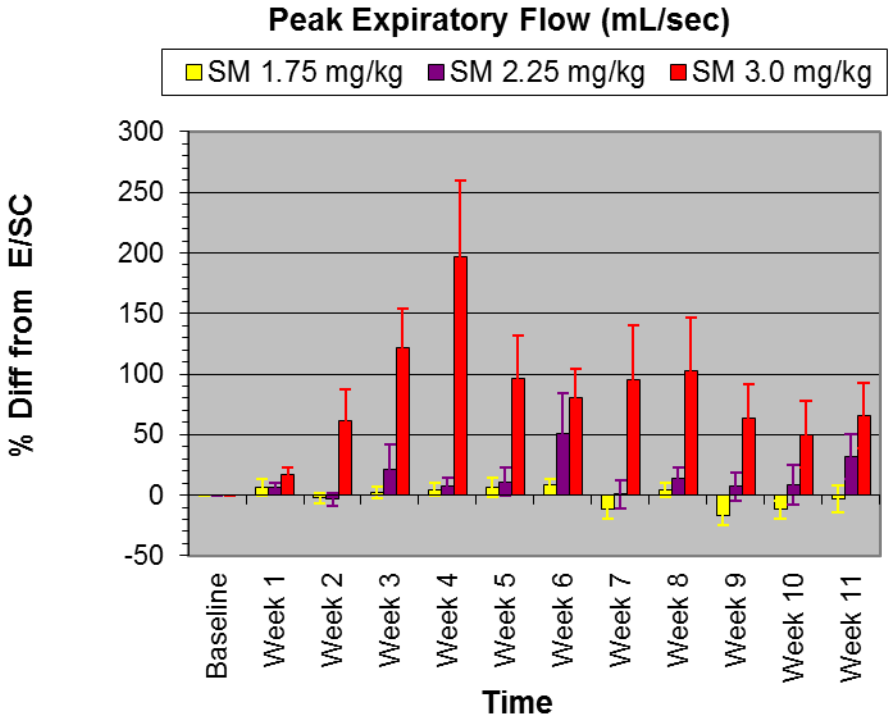

Figure 8B. A 1- to11-week profile of the effects of inhaled aerosolized SM on peak expiratory flow. Data shown as percent difference from ethanol/saline controls.

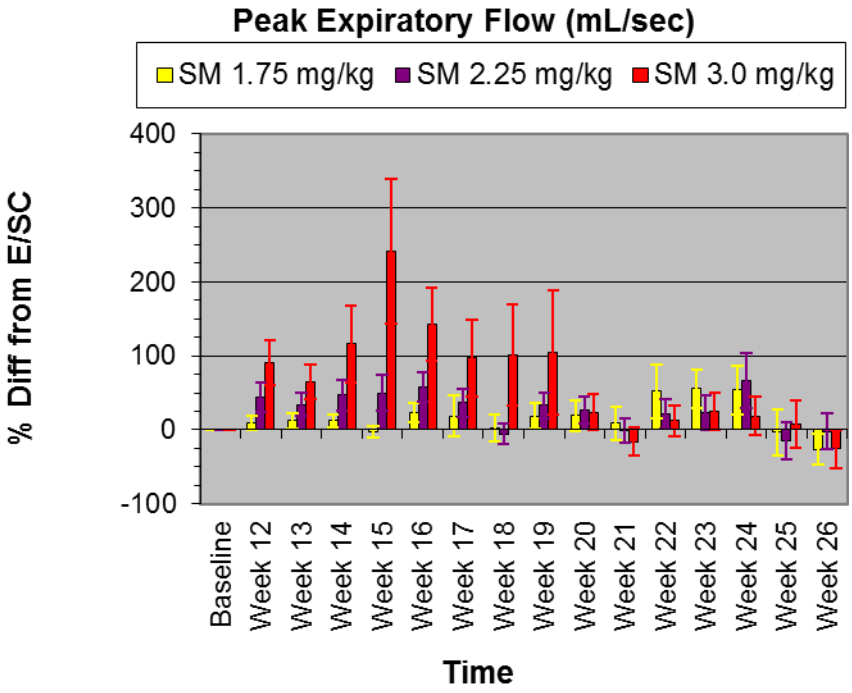

Figure 8C. A 12- to 26-week profile of the effects of inhaled aerosolized SM on peak expiratory flow. Data shown as percent difference from ethanol/saline controls.

Figure 9A shows the temporal changes in MV in SM-challenged rats. MV is the product of respiration rate (breaths/min) and tidal volume (mL). From 3-48 hrs PE a marginal increase in MV, 7-25%, was observed for all exposure doses. However, over an 11-week period the 3.0 mg/kg-dosed SM-exposed rats began to separate from the other groups, peaking at 112% vs E/SCs and then trending downward to 11 weeks PE **(Figure 9B).** During the final 15 weeks, MV peaked at week 15 in the 3.0 mg/kg groups at 100% greater than time-matched ethanol/saline controls, indicating a substantial change in respiratory function nearly 4 months PE **(Figure 9C).** The increased MV response is largely due to increased respiration rates as mention above.

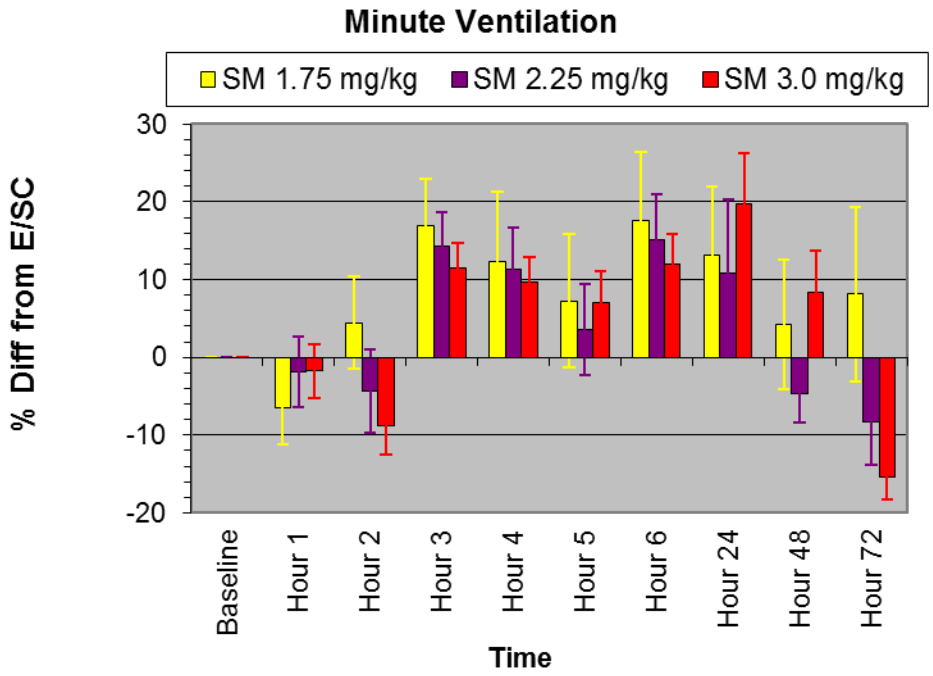

Figure 9A. A 1- to 72-hour profile of the effects of inhaled aerosolized SM on minute ventilation. Data shown as percent difference from ethanol/saline controls.

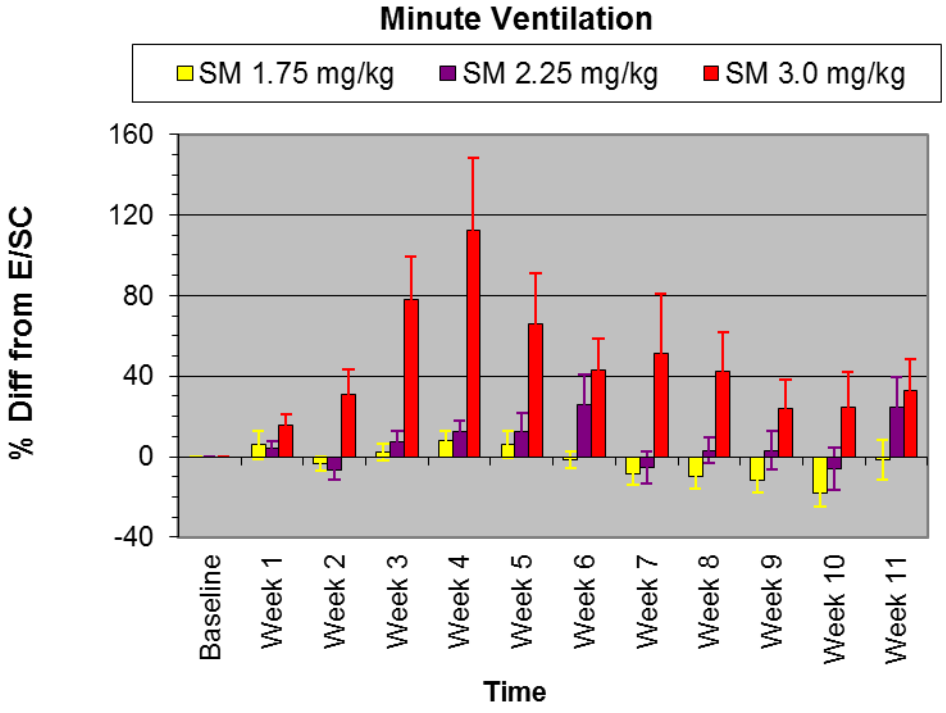

Figure 9B. A 1- to 11-week profile of the effects of inhaled aerosolized SM on minute ventilation. Data shown as percent difference from ethanol/saline controls.

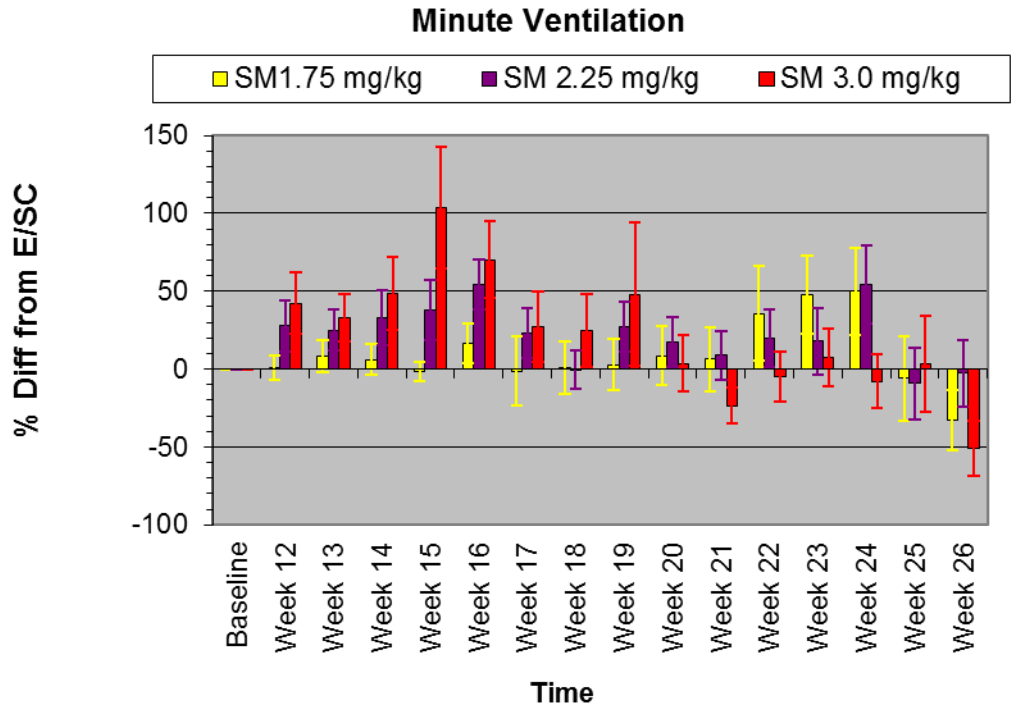

Figure 9C. A 12- to 26-week profile of the effects of inhaled aerosolized SM on minute ventilation. Data shown as percent difference from ethanol/saline controls.

A putative indicator of respiratory functional resistance, enhanced pause (EPAU) was also determined over time. It can be seen from **Figure 10A** that in the 3.0 mg/kg-exposed rats, EPAU transiently increased to 178% versus time-matched ethanol/saline controls after initially indicating a "restricted-like" condition. This could be due to the acute transient effects of SM aerosol on bronchomotor tone. During weeks 3-11 bronchoconstriction consistently increased in the 3.0 mg/kg group, which range from 60-113% higher than time-matched ethanol/saline controls **(Figure 10B).** Increased lung resistance remained higher than in controls from week 12 to week 18, indicating a persistent challenge for adequate gas exchange in the 3.0 mg/kg-dosed group **(Figure 10C).**

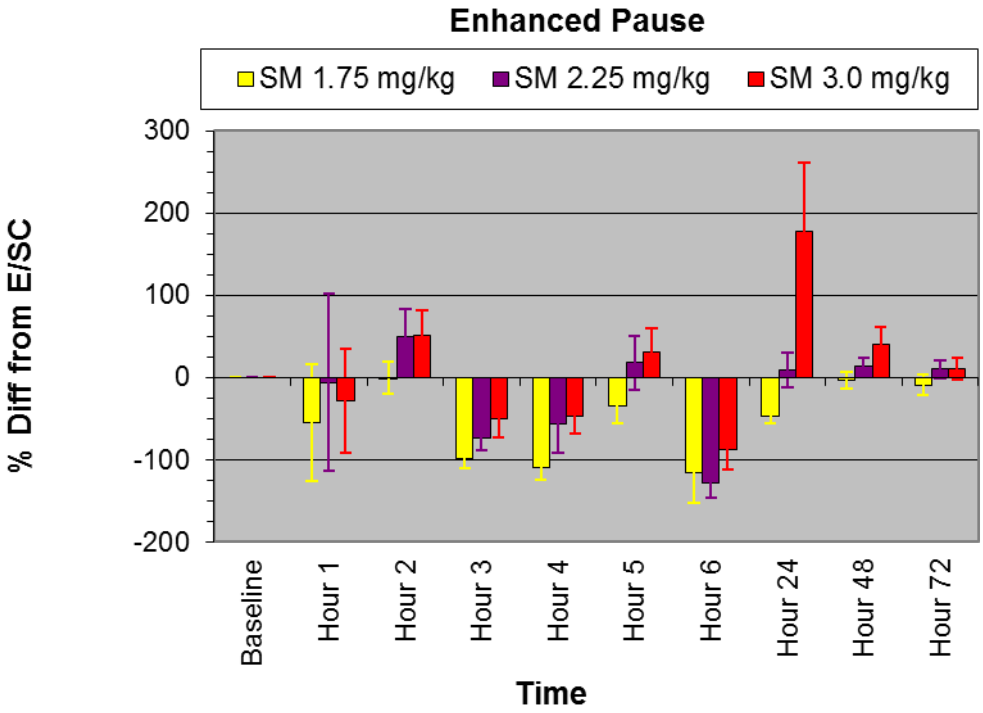

Figure 10A. A 1- to 72-hour profile of the effects of inhaled aerosolized SM on enhanced pause. Data shown as percent difference from ethanol/saline controls.

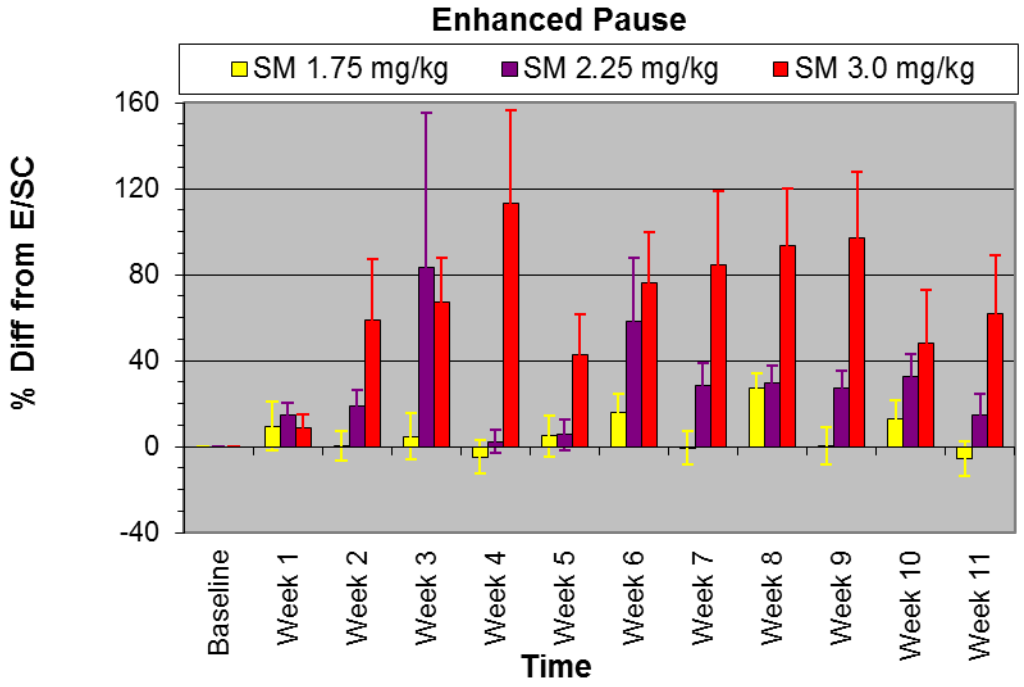

Figure 10B. A 1- to 11-week profile of the effects of inhaled aerosolized SM on enhanced pause. Data shown as percent difference from ethanol/saline controls.

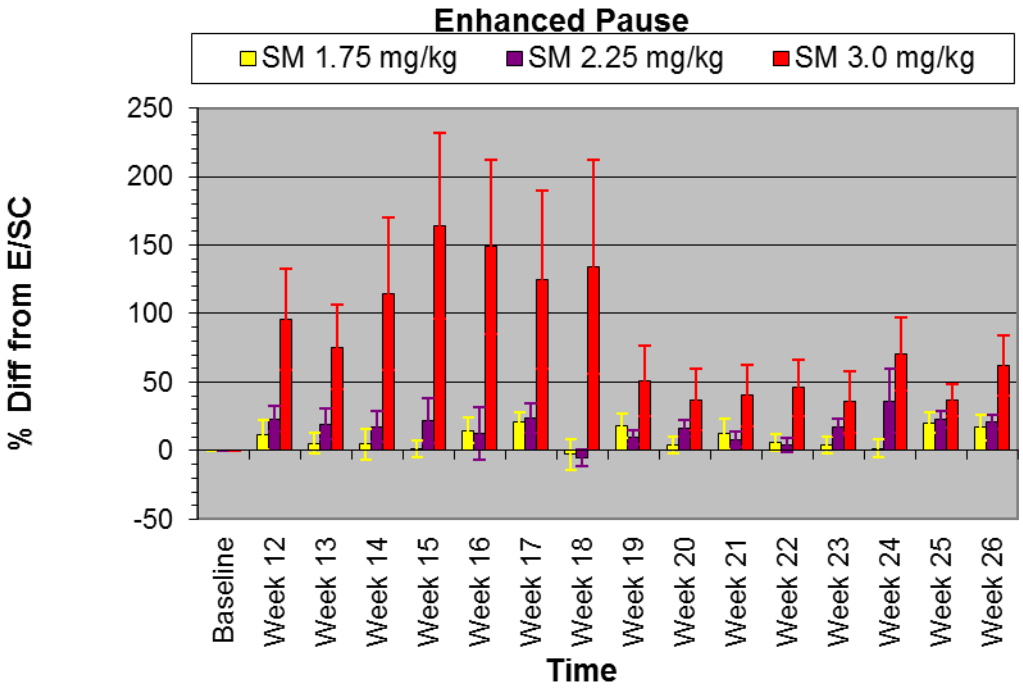

Figure 10C. A 12- to 26-week profile of the effects of inhaled aerosolized SM on enhanced pause. Data shown as percent difference from ethanol/saline controls.

BALF Protein

Lung bronchoalveolar lavage fluid (BALF) protein concentration is shown in **Figure 11.** There was a dose-dependent and temporal increase in BALF total protein in rats exposed to aerosolized SM between 24 hrs and 4 weeks PE. At 24 hrs there was a 10- and 13-fold elevation in the amount of protein in the BALF in the 2.25 and 3.0 mg/kg groups, respectively, versus time-matched ethanol/saline controls. At 4 weeks protein concentrations remained high, with 5.9- and 4.0-fold increases in the 2.25 and 3.0 mg/kg groups versus ethanol/saline controls, respectively. Furthermore, the majority of the elevated BALF protein resolved by 6 weeks PE. However, BALF protein remained elevated by 2.8-fold (544 µg/mL) in the 2.25 mg/kg-exposed group versus time-matched ethanol/saline controls at 3 months. At 6 months, there was a1.9-fold increase for 3.0 mg/kg (551 µg/mL) when compared with ethanol/saline controls (293 µg/mL). Yet the detection of increased BALF protein does not differentiate between proteins released from damaged peripheral regions of the lung versus those released from the distinct pathological damage in the upper airways. However, based on histopathology results, we concluded that there was a breach in the air/blood barrier, especially as PE time and exposure concentration increased. These results are supported by the observation that BALF LDH activities **(Figure 12)** mirrored the increases in BALF total protein **(Figure 11)** especially within the 24 hrs to 4 weeks PE time-frame. Across that same time interval, the average total LDH for the 2.25 mg/kg group was 712 IU/L versus 78 for ethanol/saline controls, a 9.1-fold increase versus only a 1.6-fold change for the 3.0 mg/kg SM group.

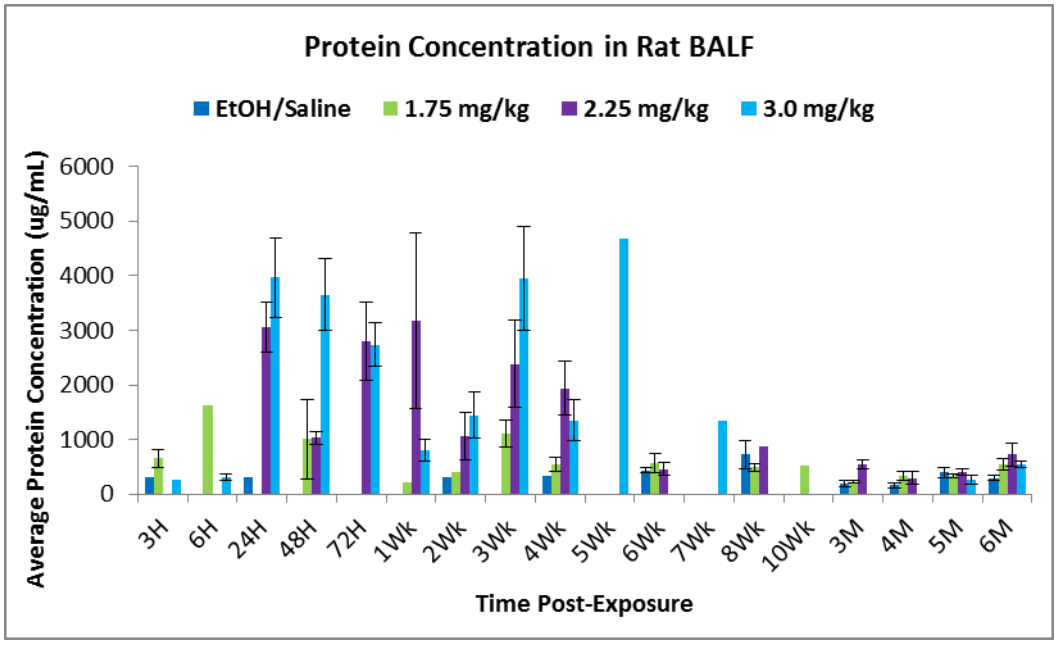

Figure 11. The temporal dose-response effects of SM exposure on BALF protein.

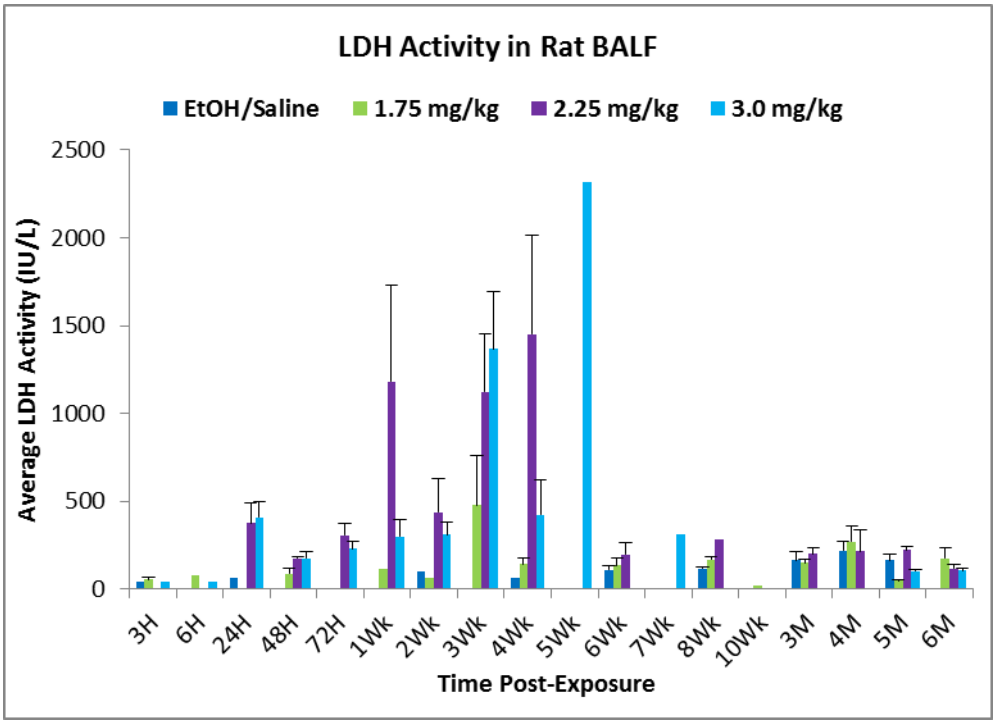

Figure 12. The temporal dose-response effects of SM exposure on BALF lactate dehydrogenase activity.

BALF Redox Response Elements (RREs)

SM inhalation caused changes in BALF RREs after a single 10-minute exposure. SM affected the free radical redox detoxification pathway involving GPx **(Figure 13),** GSH **(Figure 14)** and CAT **(Figure 15).** GPx increased approximately 9- to 40-fold at 4 weeks after SM exposure for concentrations ranging from 1.75 to 3.0 mg/kg, respectively, and increased 12- to 18-fold for all CAT SM concentrations compared to time-matched ethanol/saline controls. CAT and MPO showed the greatest number of dose and time interval changes on the animals available for sampling. The GSH redox cycle appeared to be affected only at the 6-month time point with fold changes ranging from 2.6- to 4-fold higher for all SM-exposed groups **(Figure 14).** MPO increased substantially for the 3.0 mg/kg group 24 hrs to 3 weeks PE reaching peak activity of 3400 at 24 hrs. There was a spike in MPO activity at the later time points from 3 to 6 months PE for most of the exposure concentrations **(Figure 16).** These data suggest that there is not only a possible acute neutrophilic exposure-response effect to SM, but a latent component as well that may be associated with recurrent lung damage, which could be reflective of increased neutrophil activity.

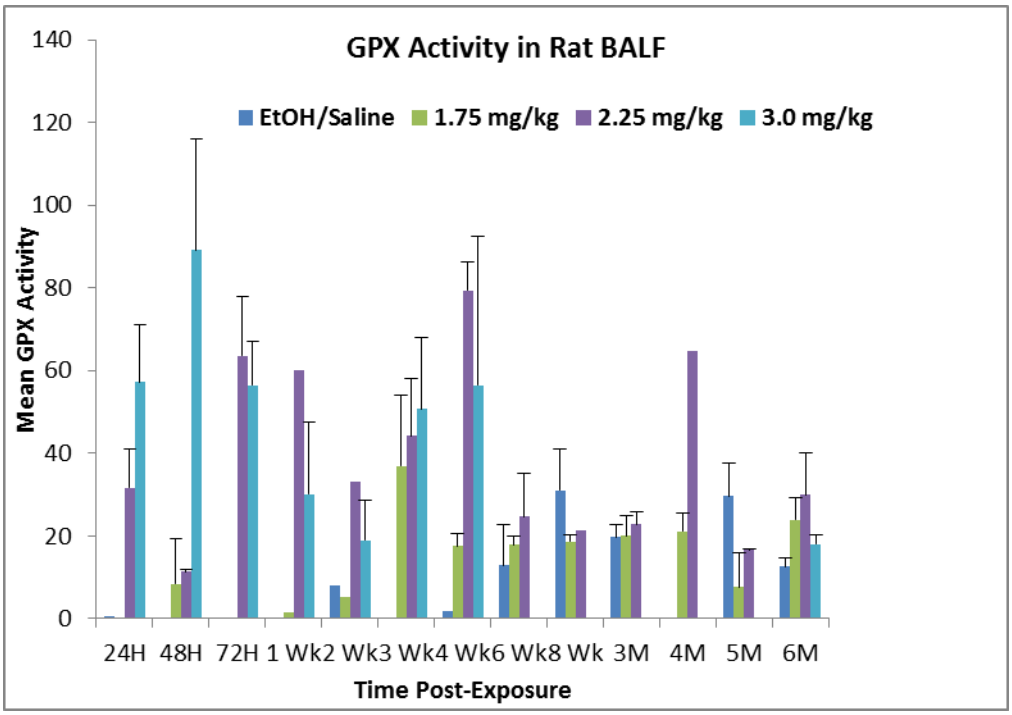

Figure 13. The temporal dose-response effects of SM exposure on BALF glutathione peroxidase activity.

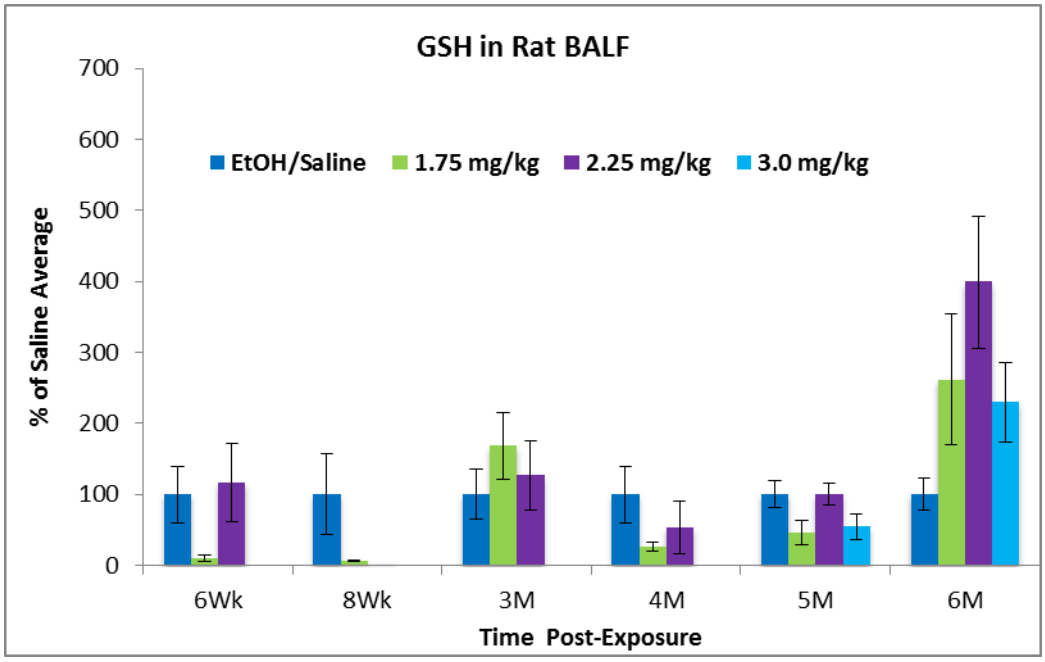

Figure 14. The temporal dose-response effects of SM on BALF total glutathione.

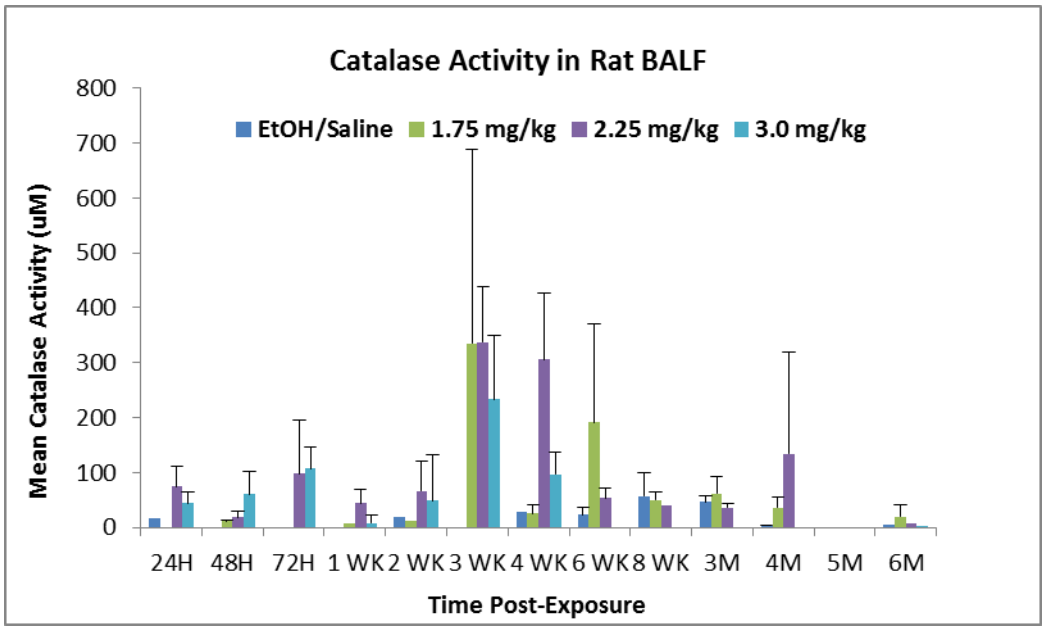

Figure 15. The temporal dose-response effects of inhaled SM on BALF catalase activity.

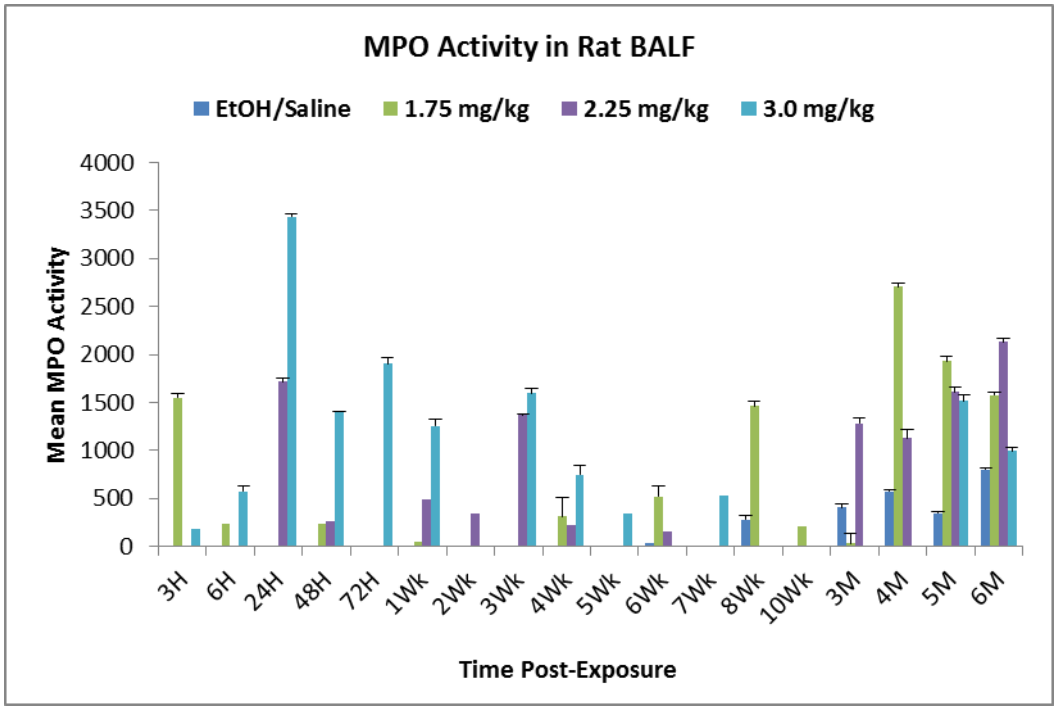

Figure 16. The temporal dose-response effects of inhaled SM on BALF myeloperoxidase activity.

Markers of Inflammation

The temporal production of IL-1α into the BALF is shown in **Figure 17.** Within the first 24 hrs the ratio of IL-1α in the 2.25 mg/kg or 3.0 mg/kg exposure groups to time-matched ethanol/saline controls increases from 15- to 29-fold, respectively. This indicated that pro-inflammatory processes were present in the internal milieu of the SM-damaged lung. There was another peak in IL-1α output at two weeks PE, then again at 5 months where IL-1α in the 2.25 mg/kg-dosed group was 28-fold greater than in the ethanol/saline controls reaching a peak level of 107±71 pg/mL, whereas in the 3.0 mg/kg group the effect was a less substantial, 7-fold greater than ethanol/saline controls, suggesting another surge in pro-inflammatory release.

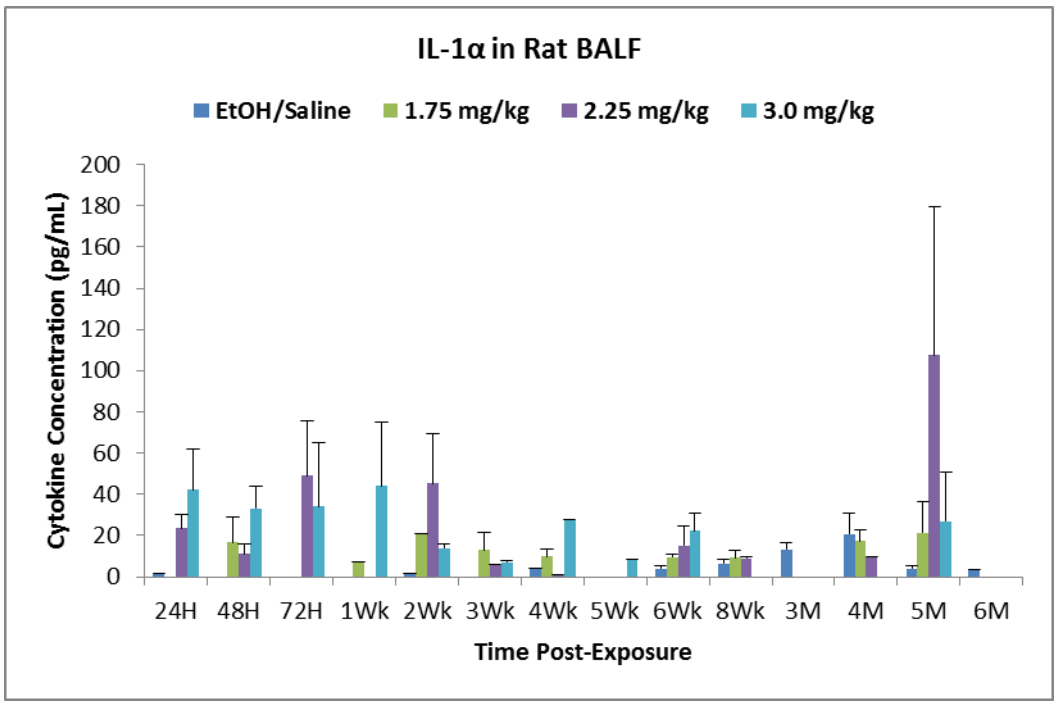

Figure 17. The temporal dose-response effects of inhaled SM on BALF cytokine IL-1α.

The cytokine IL-1β is also a marker of inflammation. The effects of inhaled SM on BALF over time for IL-1β are shown in **Figure 18.** By 24 hrs PE, IL-1β was markedly increased reaching 11- and 52-fold higher levels than time-matched ethanol/saline controls for 2.25 and 3.0 mg/kg, respectively. At 48 and 72 hrs BALF levels reached 1042 and 897 pg/mL, respectively, indicating a condition of inflammation that remained to 6 weeks PE where there was a 20-fold increase versus ethanol/saline controls. It is interesting to note that in survivors of the lower SM exposure dose, 1.75 mg/kg, a pattern of inflammation was present that was not observed at earlier time points especially at 4 and 6 months PE where 4.7- and 79-fold increases over ethanol/saline controls were detected, respectively.

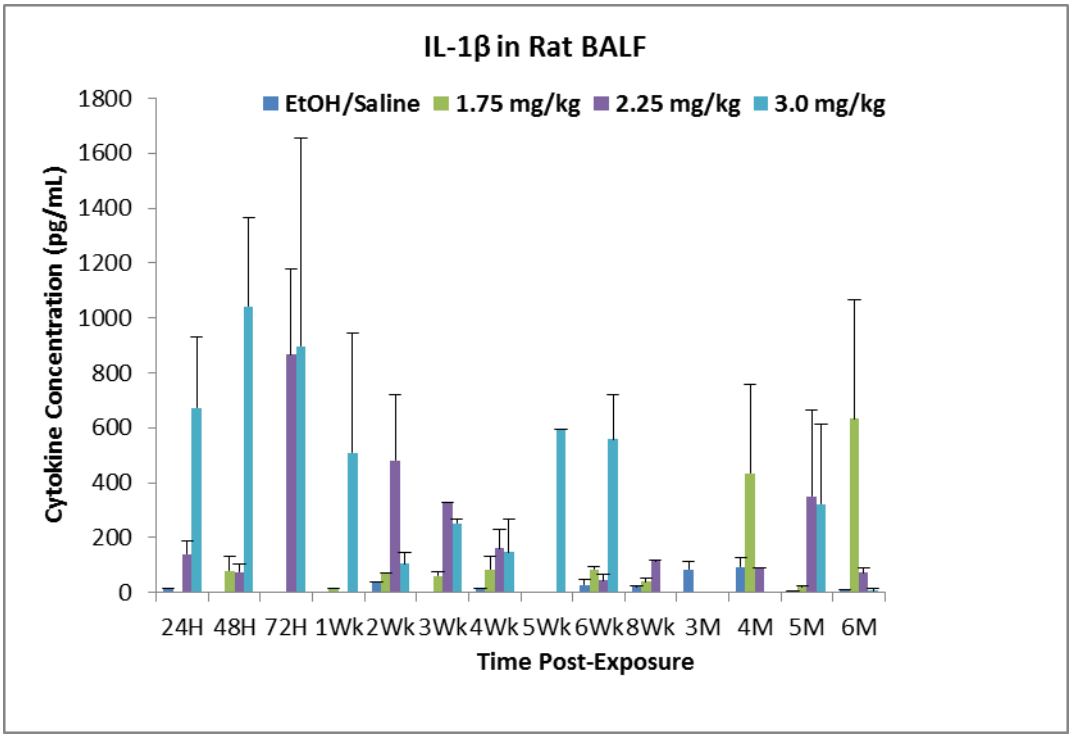

Figure 18. The temporal dose-response effects of inhaled SM on BALF cytokine IL-1β.

The chemokine GRO/KC is a marker of both inflammation and wound healing. In **Figure 19** at 24 hrs PE, there was a marked 6- to 8-fold increase of GRO/KC in the BALF for 3.0 and 2.25 mg/kg groups, respectively, compared to time-matched ethanol/saline controls. For the 2.25 mg/kg group there was an increasing trend in GRO/KC from 24 hrs to two weeks PE, reaching a maximum of 536±233 pg/mL, which was a 6.3-fold increase over time-matched ethanol/saline controls. The 3.0 mg/kg-exposed animals showed an increasing trend in GRO/KC levels from about 4-6 weeks and 5 months PE, peaking at 643±455 pg/mL, which is a 10-fold increase over time-matched ethanol/saline controls. GRO/KC showed an increasing biphasic trend early, and then again at 4 and 6 months in the 1.75 mg/kg SM-exposed rats, which suggests the recurrence of an attempt at wound healing/inflammation. Dendritic cell, epithelial cell, and bone marrow-secreted cytokine IL-7 levels are shown over time in **Figure 20**. At the earliest time point, SM exposure induced an approximately 4- to 8-fold increase in BALF IL-7 concentration as a result of exposure to 3.0 or 2.25 mg/kg, respectively, compared to time-matched ethanol/saline controls. The responses to a single 10-minute exposure were 9- to10-fold in the 1.75 and 2.25 mg/kg groups, respectively, at 5 months PE. At 6 months PE, fold changes versus time-matched ethanol/saline controls increased to 11- and 16-fold for the 1.75 and 2.25 mg/kg, respectively.

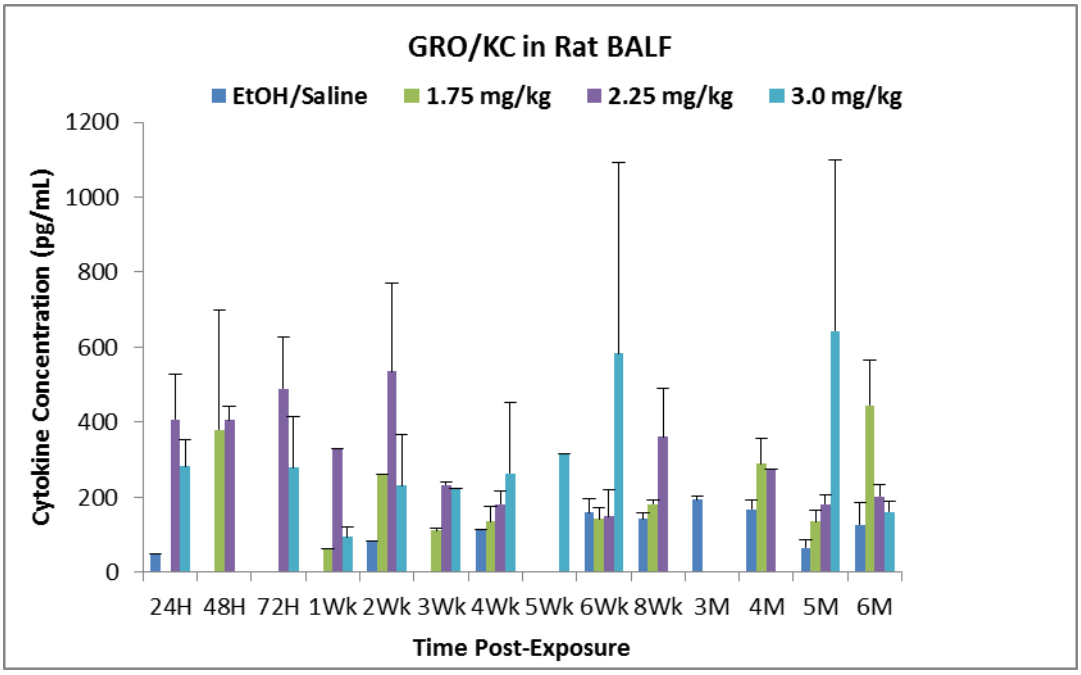

Figure 19. The temporal dose-response effects of inhaled SM on BALF chemokine GRO/KC.

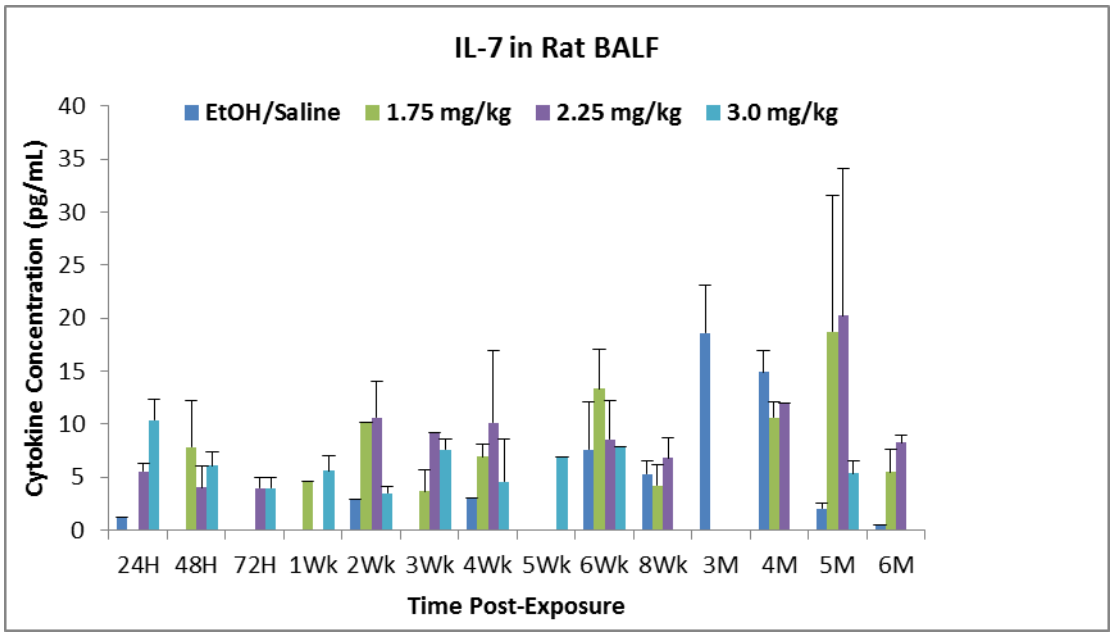

Figure 20. The temporal dose-response effects of inhaled SM on BALF cytokine IL-7.

Table 2 provides a 6-month profile of BALF inflammatory mediators totaled for each inhaled SM concentration. Our rationale was that attempting to plot the results for each exposure concentration for each time point would not adequately provide an indication of the larger SM-induced exposure-response effects totaled over time. We measured the magnitude of SM inhalation on the cumulative average concentrations of IL-5, IL-6, TNFα, IL-17 and for two chemotactic cytokines, MIP-1α and MIP-3α, for each SM exposure challenge. There was a trending temporal dose-response effect for MIP-1α, MIP-3α, IL-5, and IL-6 compared to cumulative ethanol/saline control values with fold changes in the 3.0 mg/kg group that ranged from 10.1, 5.8, 14.7, and 8.2, respectively. TNFα results indicate a possible dose-response, but a single high value was responsible for the increased change, 8.3-fold increase, for 2.25 mg/kg group, thus interfering with a true dose-response effect. IL-17 data indicate that the largest effect in fold changes was for the 1.75 mg/kg exposure concentration, which was also due to several high individual responses over time. IL-12 shows a trending concentration-dependent decrease over 6 months with a maximum decrement of 53% for the 2.25 mg/kg SM group. There were no differences in fold changes between IL-2, IL-4, IL-10, IL-13, IL-18, M-CSF, VEGF, RANTES, or EPO vs 6 month ethanol/saline controls.

TABLE 2. Fold changes in expression of average aggregate IL-5, IL-6, IL-12, IL-17, TNFα, and the chemotactic cytokines MIP-1α, MIP-3α levels in rat BALF for each SM exposure concentration over six months. Sample sizes range from 25-47/exposure concentration. Ethanol/saline controls are shown as E/SCs.

SM exposure concentration	MIP-1α (pg/mL)	Fold-changes vs E/SCs	MIP-3α (pg/mL)	Fold-changes vs E/SCs	IL-17 (pg/mL)	Fold-changes vs E/SCs
E/SCs	31		22.1		1.3	
1.75 mg/kg	65.6	2.1	79.3	3.6	11.6	8.9
2.25 mg/kg	116.4	3.8	86.0	3.9	7.5	5.8
3.0 mg/kg	314.6	10.1	128.8	5.8	8.9	6.8

SM exposure concentration	IL-12 (pg/mL)	Fold-changes vs E/SCs	IL-6 (pg/mL)	Fold-changes vs E/SCs	IL-5 (pg/mL)	Fold-changes vs E/SCs	TNF-α (pg/mL)	Fold-changes vs E/SCs
E/SCs	9.8		42.5		15.7		6.7	
1.75 mg/kg	8.7	0.89	68.7	1.6	38.1	2.4	13.7	2.0
2.25 mg/kg	4.6	0.47	308.4	7.3	55.2	3.5	58.1	8.7
3.0 mg/kg	6.7	0.68	348.6	8.2	231.5	14.7	25.6	3.8

Histopathology

At time points analyzed, the most noteworthy pulmonary and tracheal histologic lesions were seen in those animals challenged with higher doses, particularly in the 2.25 mg/kg and 3.0 mg/kg groups, although changes were present in lower-dosed animals as well. Even among the highest exposure group, however, significant histologic lesions were not always present, nor were all lung lobes equally affected. While showing no absolute restriction to a specific lobe or lobes, the most striking changes were generally seen in the right middle, right caudal, and left lobes in association with the respiratory epithelium and sub-epithelium of the conducting airways that included the trachea, intrapulmonary bronchi (absence of cartilage, but close association to bronchus-associated lymphoid tissue-BALT), and primary bronchioles. For the purpose of consistency and organization, "mainstem bronchioles" will be used to denote the changes observed in the intrapulmonary bronchi and primary bronchioles unless otherwise specified. Neither the tracheal bifurcation nor the extra-pulmonary bronchi was submitted for examination in this study and, therefore, were not examined histologically. Histologic lesions were present in the centroacinar region (terminal bronchioles and alveoli) but lessened in severity towards the periphery of the lobe.

Compared to ethanol/saline controls at 3-6 hrs PE **(Figure 21A),** multifocal individual tracheal epithelial necrosis was the most noteworthy histologic change **(Figure 21B)**. Subepithelial hemorrhage and cellular debris with neutrophilic inflammation were seen occasionally, along with individual chondrocyte necrosis. A cellular exudate composed of inflammatory cells and sloughed epithelial cells could be found in the tracheal lumen.

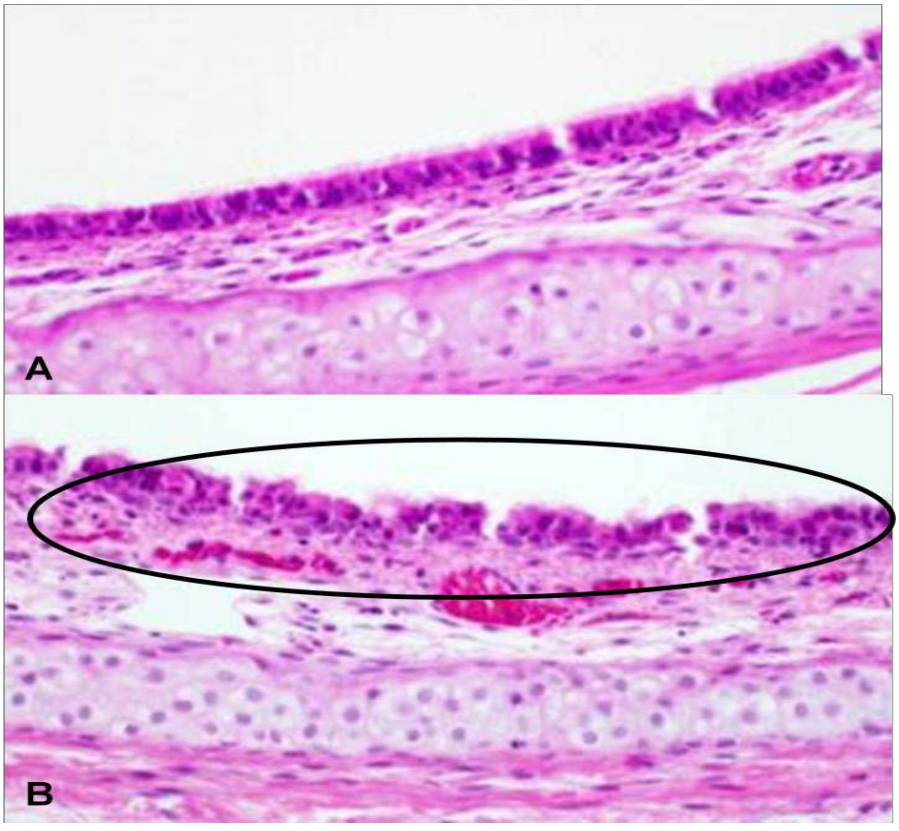

Figure 21. Morphologic changes in the trachea following SM exposure at 7.5 hours (3.0 mg/kg). (A) Normal tracheal epithelium from a non-SM-exposed Sprague Dawley rat. 40x. **(B**) In the SM-exposed animal are numerous individual and nests of shrunken epithelial cells with hypereosinophilic cytoplasm and pyknotic or karyorhectic nuclei (consistent with epithelial necrosis). 40x.

Severe bronchiolar-associated lymphoid tissue (BALT) lymphocytolysis, as early as 3 hrs and extending to 72 hrs, was seen in some but not all animals. When BALT lymphocytolysis was present, the adjacent airway epithelium was generally affected, consisting of focally extensive individual (single-cell) bronchiolar epithelial necrosis; the remaining bronchiolar epithelium was histologically normal **(Figure 22).** The occurrence of BALT is a consequence of active pulmonary inflammatory processes (Bánfi *et al.*, 2009).

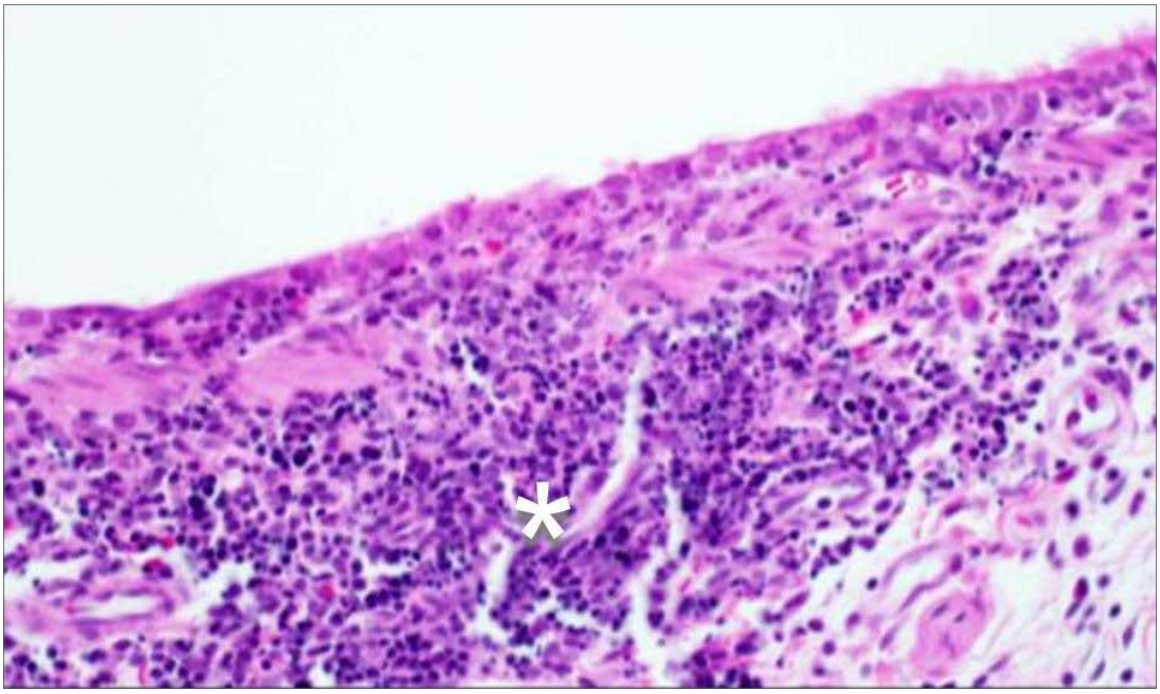

Figure 22. Morphologic changes in the accessory lobe following SM exposure at 7.5 hours (3.0 mg/kg). Histopathology of the BALT and overlying respiratory epithelium in the accessory lung lobe. Note the "rounded-up" lymphoid cells (*), consistent with extensive lymphocytolysis, and the individual necrotic epithelial cells. 40x.

By 24 hrs and extending through 72 hrs for the 3.0 mg/kg SM groups, brightly eosinophilic fibrillar and cellular pseudomembranes occasionally formed along the denuded surface and partially occluded the tracheal lumen **(Figure 23A)**. Greater than 50% of the tracheal epithelium was affected with one or more of the following changes: single cell and nests of necrotic epithelial cells, clefting/separation from the basement membrane **(Figure 23B)**, and ulceration. Subepithelial hemorrhage and inflammation and individual chondrocyte necrosis **(Figure 23C)** were also more extensive. In the lungs, individual bronchiolar epithelial necrosis became more apparent with occasional fibrinous and cellular exudation and pseudomembrane formation in the secondary bronchi and mainstem bronchioles **(Figures 24A and B)** following 2.25 mg/kg SM challenge. At 72 hrs (data not shown), there was a mild increase in bronchiolar goblet cells which progressively became more noticeable between 7 and 14 days post-challenge. Additionally, in other areas, there was attenuation of the bronchiolar epithelium.

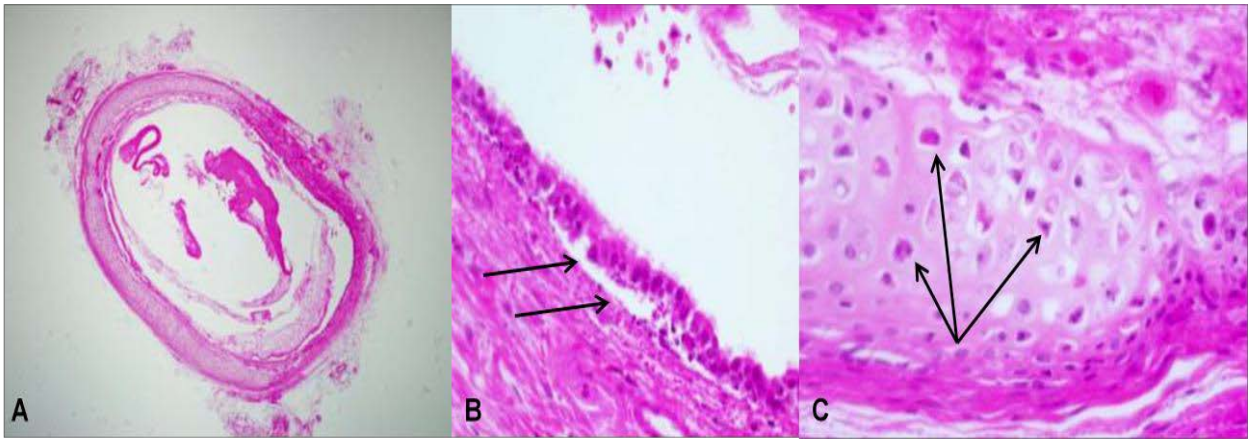

Figure 23. Histomorphologic changes in the trachea following a 3.0 mg/kg SM exposure at 24 hours. (A) A fibrinous and cellular pseudomembrane and plug partially occlude the tracheal lumen. 4x. **(B)** Separation and clefting of necrotic epithelium from the underlying basement membrane (arrows)**.** 40x. **(C)** Numerous brightly eosinophilic and necrotic chondrocytes are present in the tracheal cartilage (arrows). 60x.

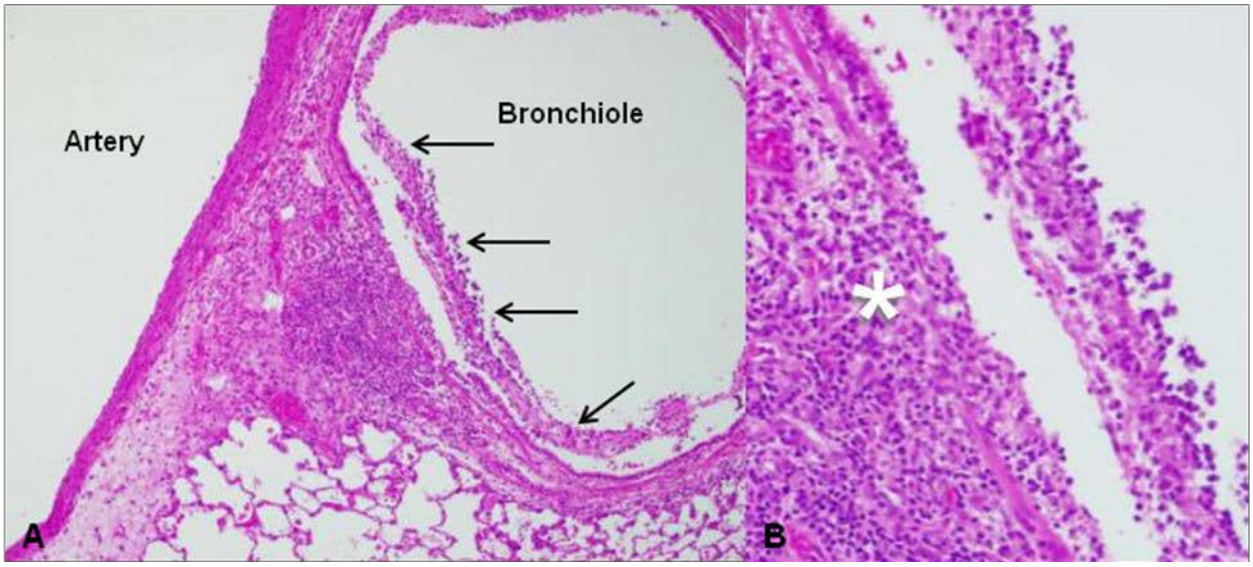

Figure 24. Histomorphologic changes in the left lobe following SM exposure at 48 hours (2.25 mg/kg). (A) A fibrinous and cellular exudate and pseudomembrane partially (arrows) occlude the bronchiolar lumen. 10x. **(B)** Note the ulceration and loss of respiratory epithelium (*) adjacent to the BALT. 20x

Transmigration of a few neutrophils through the bronchiolar epithelium and periobronchiolar connective tissue was also noted as early as 24 hrs. Within the terminal bronchioles and alveoli, alveolar histiocytosis, characterized by 2-4 mononuclear cells (macrophages) with abundant eosinophilic vacuolated cytoplasm, was common, although a mixed neutrophilic exudate was occasionally observed. Other early findings observed in the most affected lung

lobes included alveolar (luminal) edema, alveolar interstitial edema and inflammation, alveolar epithelial cell hypertrophy, and, rarely, alveolar hemorrhage and fibrin **(Figures 25A-C).**

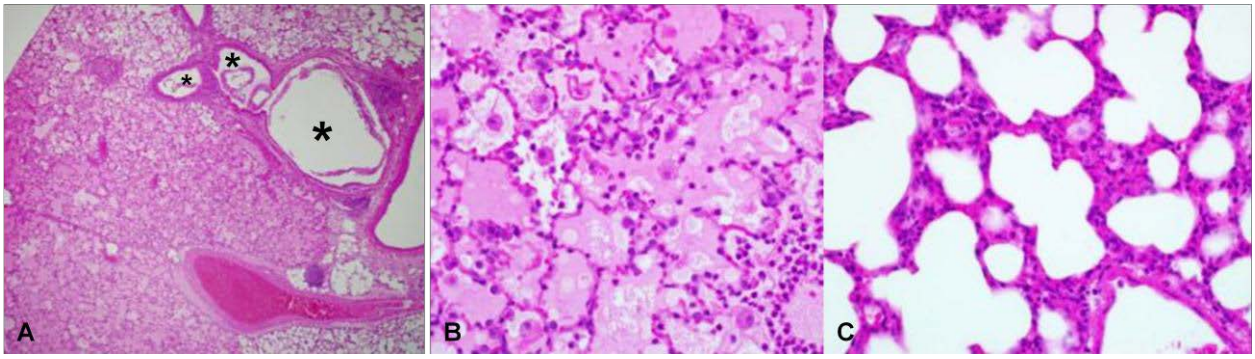

Figure 25. Histomorphologic changes in the left lobe and right cranial lobe following SM exposure at 48 hours (2.25 or 3.0 mg/kg). (A) Severe alveolar proteinaceous edema and flooding adjacent to the mainstem bronchioles. Note the fibrinous and cellular exudate that partially occludes the bronchiole lumen (*). 4x. **(B)** Proteinaceous edema admixed with variable numbers of foamy alveolar macrophages and non-degenerate neutrophils fill the alveolar lumina. 40x. **(C)** Although there is no evidence of alveolar edema or exudation, the alveolar interstitium is expanded 3-4x normal by neutrophilic and histiocytic inflammation and edema. 40x.

Between 2-3 weeks after SM challenge, focally extensive sub-epithelial proliferations of loosely packed fibroblast-like cells elevating the ulcerated bronchiolar epithelium were observed in the mainstem bronchioles of a few animals **(Figures 26A-B)**. Bronchiolar epithelial necrosis, ulceration, and loss with attenuation and/or goblet cell hyperplasia (often in the same airway) were more common findings. A fibrinous and cellular bronchiolar exudate (with occasional hemorrhage) was also observed. Although minor edema was present, alveolar neutrophilic exudate was more common and occasionally admixed with hemorrhage and fibrin. Neutrophilic and histiocytic alveolar interstitial inflammation and alveoli lined by plump epithelial cells (suggestive of type II hyperplasia) were accompanying histologic lesions. In a few areas, rare foci of spindled cells (focal alveolar fibrosis) also mildly expanded the alveolar interstitium. The tracheal epithelial changes resembled those seen in the mainstem bronchioles, although individual chondrocyte necrosis was not as readily observed.

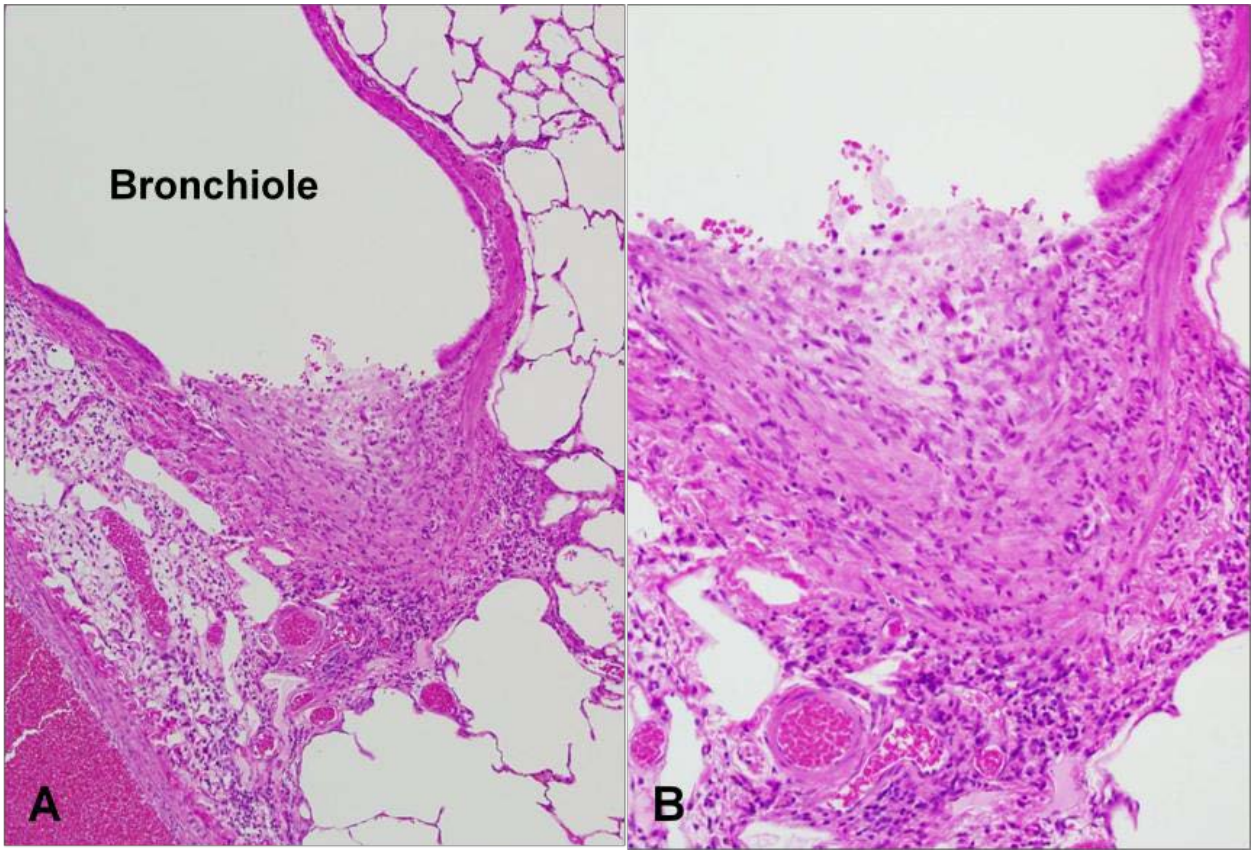

Figure 26. Histomorphologic changes in the left lobe following SM exposure at 21 days (3.0 mg/kg). (A, B) The bronchiolar subepithelial proliferation composed of fibroblast-like cells admixed with few inflammatory cells elevates the ulcerated epithelium. 10x, 20x.

Although lesions were observed at earlier time points, the most widespread and generally the most severe lesions were present between 4 and 7 weeks following a 2.25 mg/kg SM exposure. When present, the focal sub-epithelial proliferation became more organized, partially occluded the airway lumen, and was partially or completely lined by respiratory epithelium resembling a fibroepithelial polyp **(Figures 27A and 27B).**

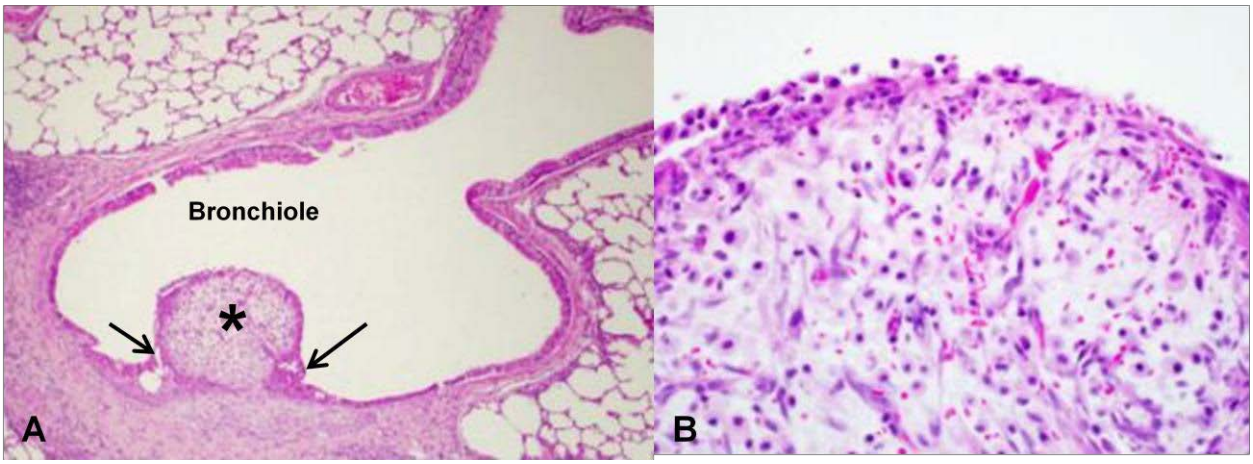

Figure 27. Histomorphologic changes in the right caudal lobe following SM exposure at 31 days (2.25 mg/kg). (A, B) A well-organized, dome-shaped, ulcerated subepithelial proliferation of spindled fibroblast-like cells (*) supported by a loose edematous matrix with small caliber vessels with a mixed inflammatory infiltrate partially occludes the bronchiole lumen. Note how in the ulcerated epithelium lining the growth is contiguous with the bronchiolar epithelium (arrows). The proliferation most resembles a fibroepithelial polyp. **(A)** 4x, **(B)** 40x.

Unlike the mostly proteinaceous bronchiolar exudate, the alveolar exudate varied from predominately proteinaceous to heavily neutrophilic or a combination of both. Alveolar hemorrhage, fibrin, and hemoglobin crystals admixed with erythrocyte- and hemosiderin-laden macrophages were also routinely seen. In the most affected areas, prominent (hyperplastic) alveolar epithelial cells lined septae thickened up to 4x normal by neutrophilic and histiocytic inflammation, fibrosis, and occasionally individual cellular necrosis **(Figure 28)**. Vascular necrosis with organized fibrin thrombi, affecting small caliber vessels, was also observed in some animals. Tracheal epithelial attenuation, squamous metaplasia, ulceration, and/or loss with fibrinous and cellular exudation continued to be observed.

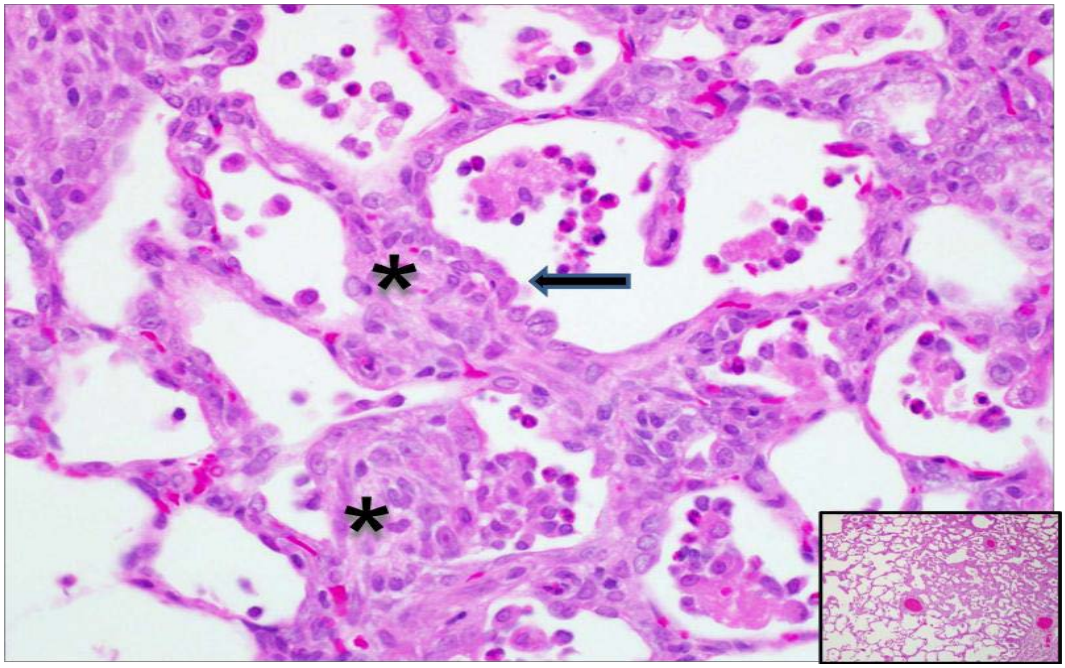

Figure 28. Histomorphologic changes in the left lobe following SM exposure at 28 days (3.0 mg/kg). Alveolar septae are markedly thickened by fibroblast-like cells and mononuclear inflammation (*) and occasionally lined by prominent cuboidal alveolar epithelial cells (arrow). An alveolar exudate composed of alveolar macrophages, neutrophils, and cellular debris partially occluding the airways. 40x. **Inset:** Note the diffuse thickening of the alveolar septae.

At 2 months PE, similar histologic lesions were seen in the lung and trachea but were generally not as severe. The most noteworthy changes were the partially or completely epithelial-lined subepithelial fibrous proliferations/polyps, bronchiolar goblet cell hyperplasia, and alveolar interstitial fibrosis **(Figures 29A and 29B).** Between 3 and 4 months, the sub-epithelial polyps and bronchiolar goblet cell hyperplasia in larger airways remained noteworthy features **(Figure 30A)**. When present, the alveolar changes were minimal to mild in severity and consisted of interstitial fibrosis and histiocytosis. Occasionally, in some lung lobe sections, alveolar spaces had united and formed dilated alveolar spaces, a histological finding consistent with emphysematous change. This finding was most noticeable adjacent to mainstem bronchioles partially occluded by the subepithelial fibrous proliferations/polyps. Additionally, sub-epithelial fibrous proliferation with osseous metaplasia was infrequently found in the trachea of some animals **(Figure 30B).** Likewise, the tracheal epithelial changes were also similar **(Figure 31),** although goblet cell hyperplasia was only occasionally detected.

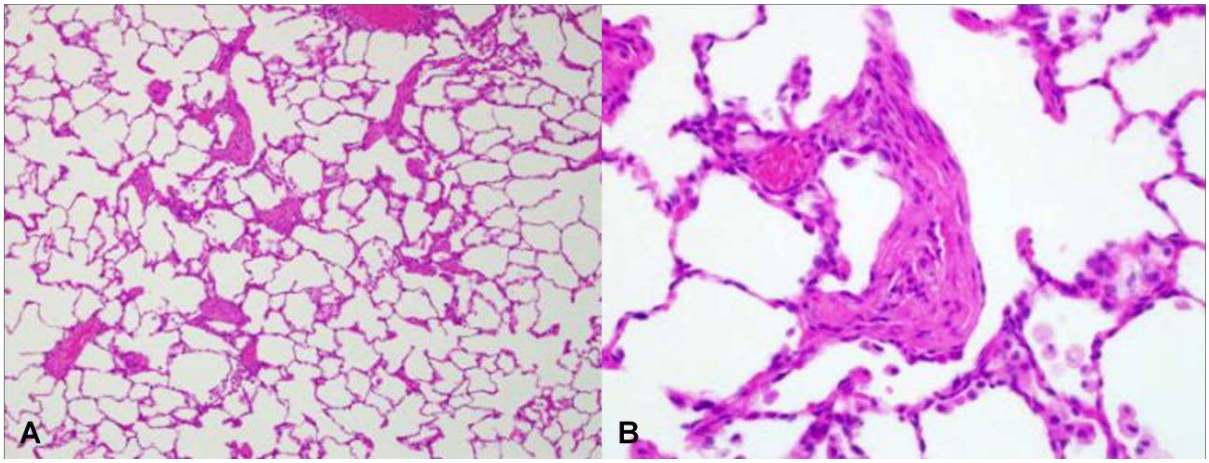

Figure 29. Histomorphologic changes in the right cranial lobe following SM exposure at 2 months (2.25 mg/kg). (A, B). Multifocal alveolar interstitial fibrosis (arrows) with minimal alveolar histiocytosis. **(A)** 10x, **(B)** 40x.

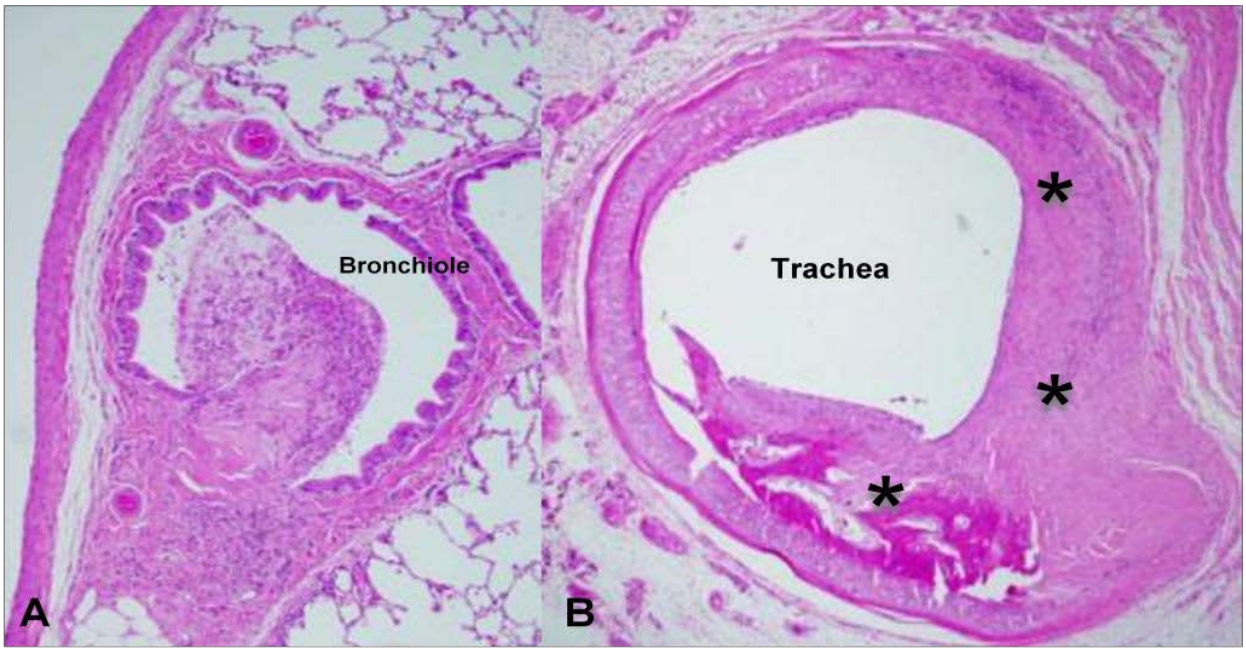

Figure 30. Histomorphologic changes in the left lobe and trachea following SM exposure at 4 months (3.0 mg/kg). (A) Approximately 50% of the bronchiole lumen is occluded by a fibroepithelial polyp. 10x. **(B)** Marked distortion of the trachea architecture by severe subepithelial fibrous proliferation and osseous metaplasia **(*). 40x.**

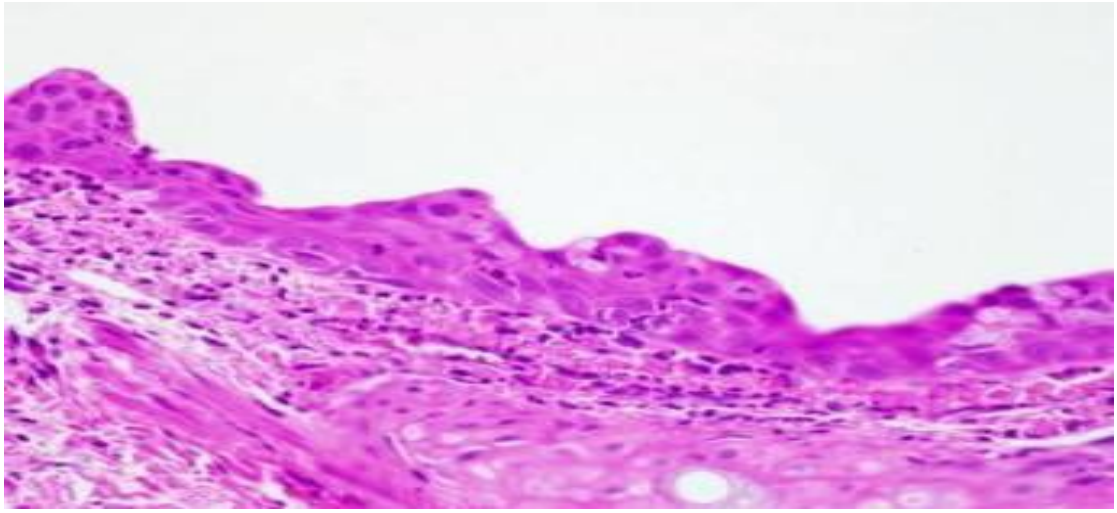

Figure 31. Morphologic changes in the trachea following SM exposure at 3 months (2.25 mg/kg). (A) Diffuse squamous metaplasia with loss of cilia and scattered necrotic epithelial cells. 40x.

Histologic pathological lesions were observed in rats exposed to 2.25 or 3.0 mg/kg SM and euthanized at the timeframes indicated**. Figures 32A-C** show scores ranging to 6 months PE with emphasis aligned to corresponding temporal changes in mortality. **Figure 32A** shows the temporal effects of SM exposure on tracheal epithelial necrosis. Exposure to SM at 3.0 mg/kg resulted in a persistent necrotic condition from 2-8 weeks after exposure, whereas exposure to 2.25 mg/kg had less of an effect, but also resulted in a chronic condition that was largely resolved in survivors out to10 weeks PE. **Figure 32B** shows a dose-dependent delayed response for bronchiolar goblet cell hyperplasia with 2.25 mg/kg peaking in the 6-week timeframe, while for 3.0 mg/kg SM dose an earlier increase for hyperplasia was observed. Perivascular edema was observed in the 2.25 mg/kg group from day 1 to nearly 10 weeks peaking at 3 and 8 weeks PE. At 3 weeks, there was a marked decrease in survival in the 2.25 mg/kg group and again at 7-8 weeks PE. A similar, but reduced, effect was seen in the 3.0 mg/kg group from 3-8 weeks also matching quite well with increased mortality **(Figure 32C).** Results at 5 months PE for the 1.75 mg/kg group showed moderate bronchiolar sub-epithelial fibrous proliferations and severe bronchiolar sub-epithelial fibrous proliferation that partially occluded the lumen. Additionally, there was evidence of perivascular hemosiderosis and severe multi-layered tracheal squamous metaplasia that extended into the lumen (pathology not shown).

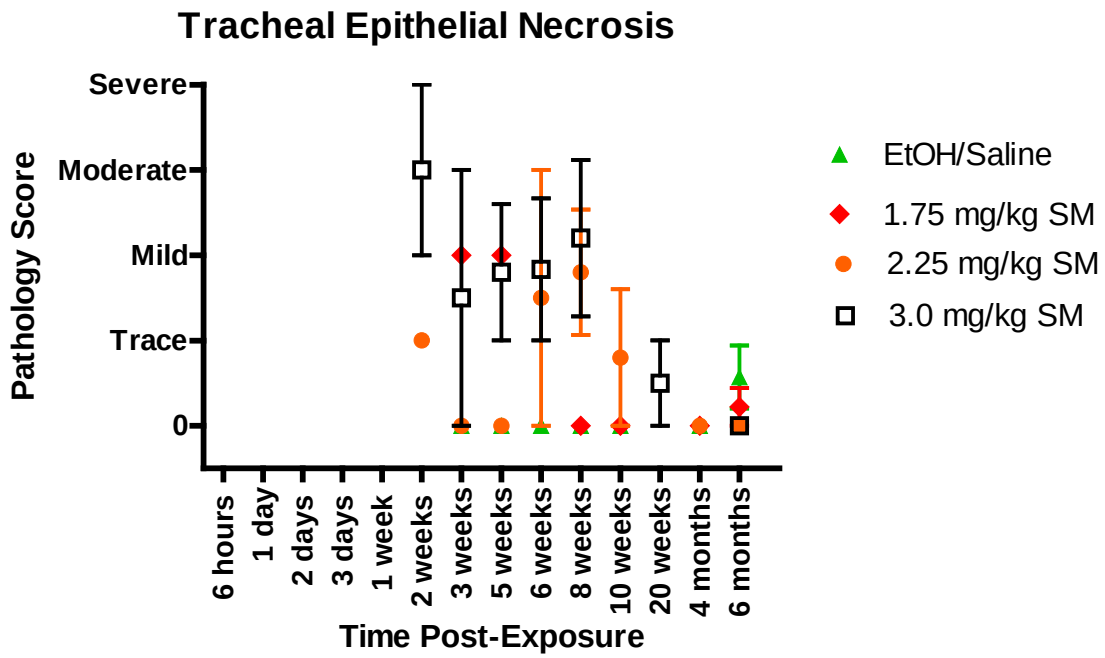

Figure 32A. The temporal dose-response effects on tracheal epithelial cell necrosis induced by exposure to inhaled aerosolized SM. Data are plotted as mean ± SEM.

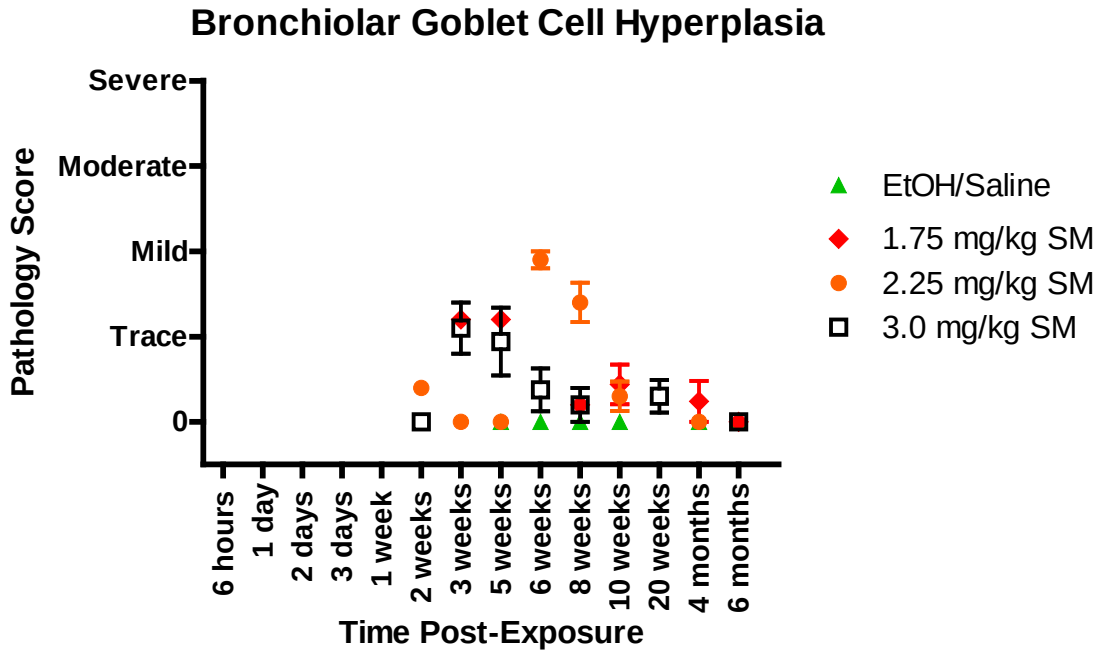

Figure 32B. The temporal dose-response effects on bronchiolar goblet cell hyperplasia induced by exposure to inhaled aerosolized SM. Data are plotted as mean ± SEM.

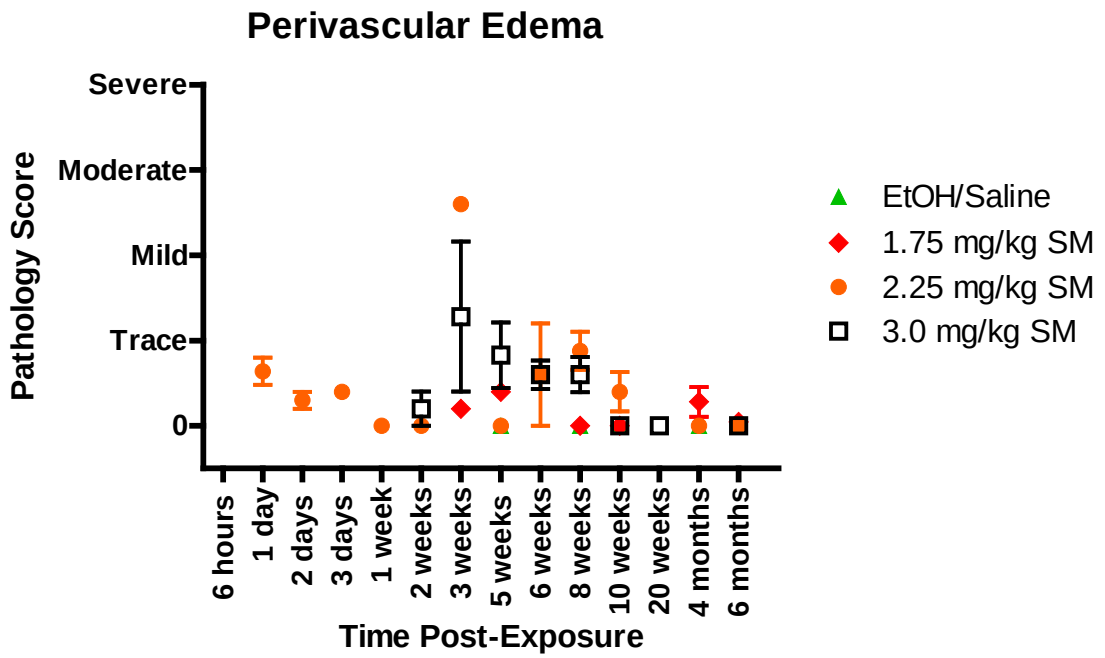

Figure 32C. The temporal dose-response effects on bronchiolar perivascular edema induced by exposure to inhaled aerosolized SM. Data are plotted as mean ± SEM.

Mesenchymal Stem Therapy in SM-Exposed Rats

The 2.25 mg/kg dose group was chosen to test MSC therapy because the mortality rate for the group from weeks 3 to 6 was approximately 40-45%. The rationale is supported by the data in **(Table 1)** indicating that testing the high SM exposure concentration was not practical because of significant losses—70% in the 3.0 mg/kg group—over the same time interval. **Figure 33** shows that a single MSC treatment delivered 6 hrs PE to aerosolized SM reduced the mortality rate at 5 weeks compared with survival rates shown in **Figure 3** and compared with untreated 2.25 mg/kg SM-exposed rats. Lung pathology scores at five weeks after the stem cell treatment showed bronchiolar epithelial necrosis and tracheal exudates reduced to ethanol/saline controls levels (none observed). Stem cell treatment of SM-exposed animals improved survival, 21% over treatment with vehicle alone, but also delayed the onset of symptoms, compared to un-treated exposed. Treatment using MSCs significantly improved lung pathology scores compared to SM+ethanol/saline controls, p=0.001, at 5 weeks PE **(Figure 34).** Additionally, stem cell therapy and saline alone reduced the effects of a 10-minute inhalation exposure on bronchiolar goblet cell hyperplasia, bronchial epithelial cell necrosis, and tracheal exudate formation **(Figures 35A-C).**

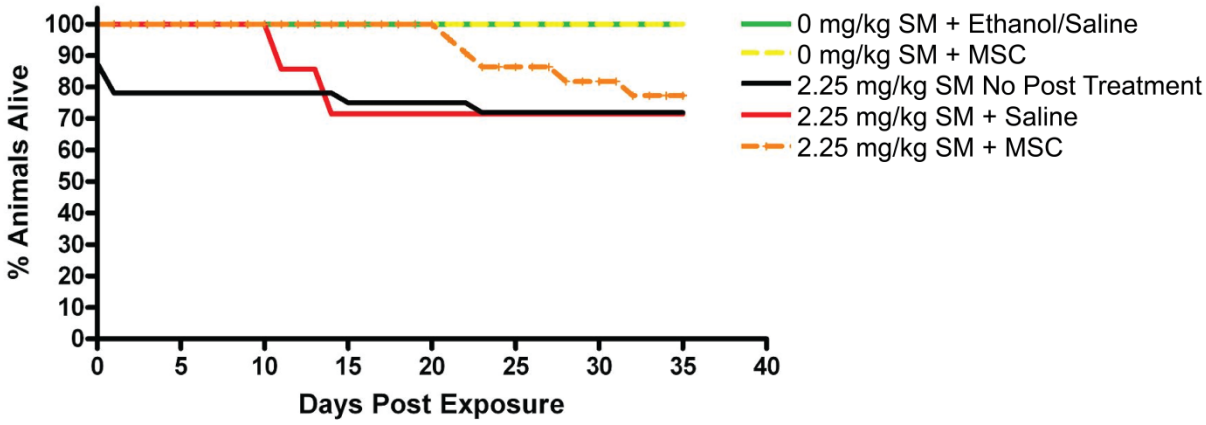

Figure 33. Kaplan-Meier plot of survival rates over 5 weeks in 2.25 mg/kg SM-exposed rats treated with and without mesenchymal stem cells.

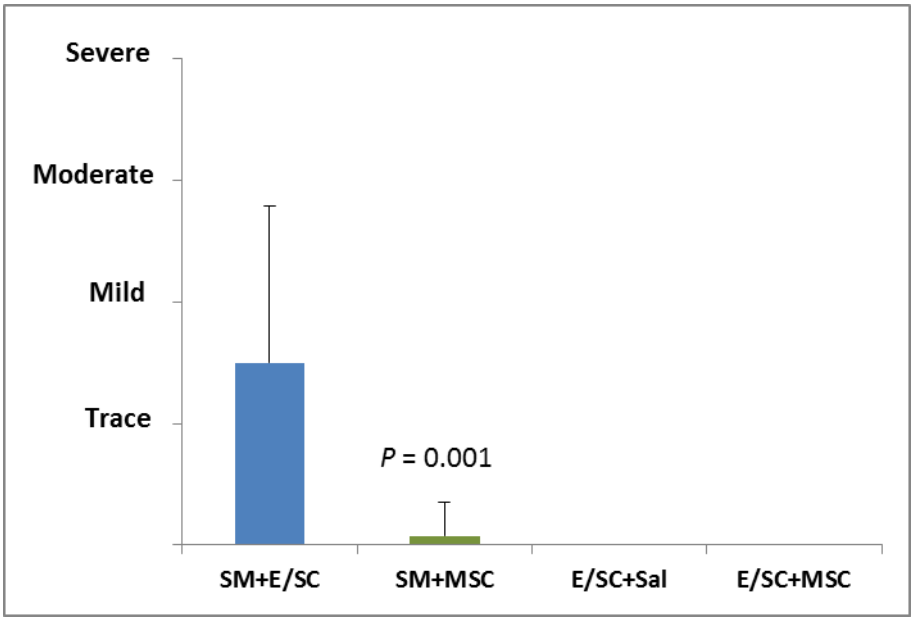

Figure 34. Lung pathology scores in E/SC animals exposed to SM with or without treatment with mesenchymal stem cells (MSCs). A single MSC treatment 6 hrs post-exposure had a significant effect on lowering pathology scores compared to scores in SM-exposed animals and treated with or without saline at 5 weeks PE. Data are plotted as mean ± SEM.

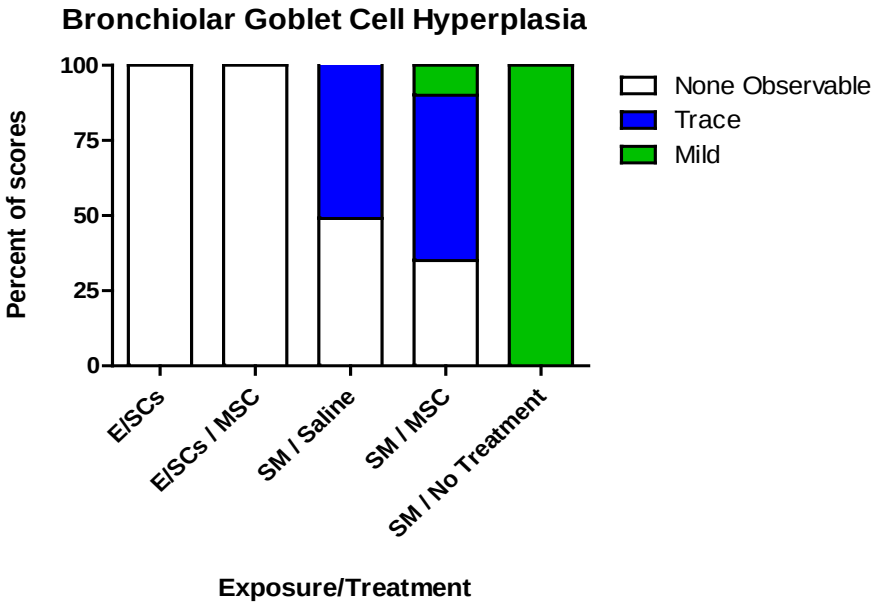

Figure 35A. The effects of 2.25 mg/kg inhaled aerosolized SM alone, saline alone, or inhaled aerosolized 2.25 mg/kg SM + MSC on bronchiolar goblet cell hyperplasia histopathology at 5 weeks post-exposure. MSCs were injected into the jugular vein at 6 hours post-SM exposure.

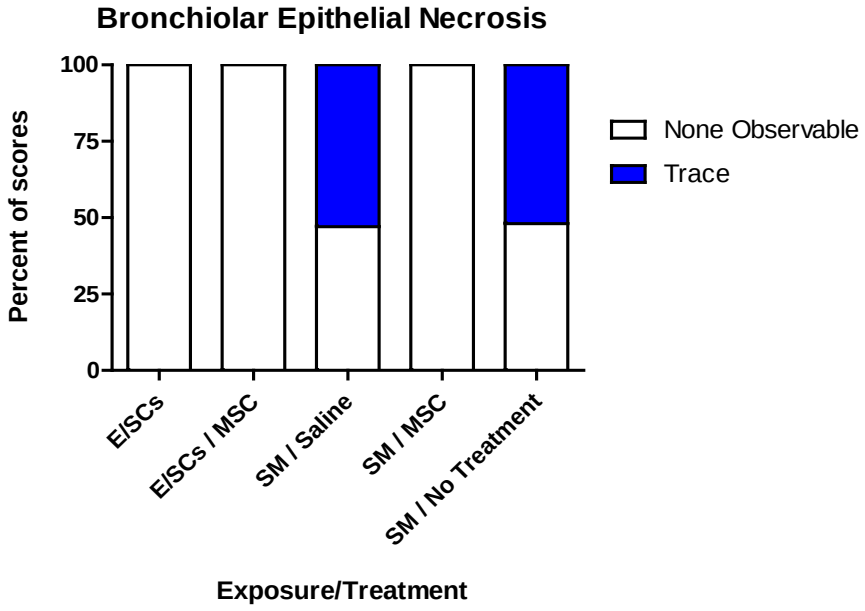

Figure 35B. The effects of 2.25 mg/kg inhaled aerosolized SM alone, saline alone, or inhaled aerosolized 2.25 mg/kg SM + MSC on bronchiolar epithelial cell histopathology at 5 weeks post-exposure. MSCs were injected into the jugular vein at 6 hours post-SM exposure.

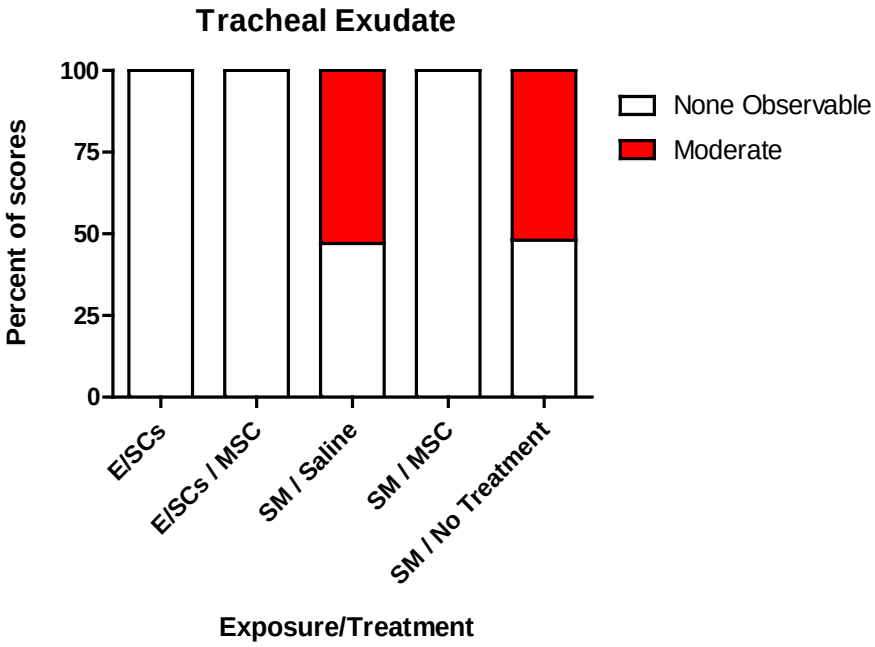

Figure 35C. The effects of 2.25 mg/kg inhaled aerosolized SM alone, saline alone, or inhaled aerosolized 2.25 mg/kg SM + MSC on tracheal exudate histopathology at 5 weeks post-exposure. MSCs were injected into the jugular vein at 6 hours post-SM exposure.

DISCUSSION

The objective of this six-month project was to determine the toxicological, physiological, histopathological, and biochemical effects on a range of response variables resulting from a single 10-minute aerosolized SM inhalation challenge in the rat. It is not surprising that SM caused an overwhelming effect on rat biology and physiology. Much of the data described herein support the published literature from humans exposed to SM during the Iran-Iraq War (Willems, 1989; Ghanei and Harandi, 2007). Several limitations of our model **(Figure 1)** are the uses of a ventilated, anesthetized rodent model, to achieve an intra-tracheal aerosol exposure challenge. The advantage was that we could control the MV, bypassing the detoxification pathways in the nasal passages thereby adapting our model to mimic mouth-breathing humans and avoiding contamination of the fur. In some SM inhalation models nose-only exposures were performed, which most likely added a nasal toxicity component to the exposure injury (Allon *et al*., 2009; Vijayraghavan, 1997). Our exposure concentrations were in agreement with previously published SM challenge exposure atmospheres (Anderson *et al*., 1996; Allon *et al*., 2009). Moreover, the validity of the use of this model was strengthened by the dose-response appearance of SM adducts measured in the blood over the initial 24 hrs, as seen in **Figure 5** to approximately 25 days PE **(Figure 6).** While these adducts are present, they are basically inactive since they are protein bound. In the current model, SM-induced mortality was clearly dose-dependent and approached 80% at 180 days PE with intervening fatality inflection points at roughly 5, 9, and 18 weeks at the highest SM concentration **(Figure 3).**

As was observed by the Iranians in human casualties many years following the Iran-Iraq War (1984-1988), pulmonary function was severely compromised in rats that survived to their experimental end-points. This was generally described as asthma, bronchiolitis, recurrent pneumonia, and chronic obstructive pulmonary disease (COPD) (Willems, 1989; Hefazi *et al*., 2005; Balali-Mood and Hefazi, 2006). COPD is characterized by persistent airflow limitation. It can be progressive and is strongly linked to a chronic inflammatory response in the airways following exposure to irritants such as gases or particles. In the current study, SM-induced compromised respiratory function was determined by WBP studies and indicated an asthma-like COPD. While a true asthmatic response is validated through the application of a methylcholine challenge, we were unable to test this in the present study. However, we observed a condition of both large airway flow obstruction **(Figures 23, 27, 30)** and gas exchange abnormalities **(Figures 4B and C)** most likely the result of ventilation/perfusion inequalities. Whereas in humans when O_2 saturations are <92%, asthma is generally diagnosed. From our data we observed that O_2 saturations were below 85% after about 6 hrs to 45 days **(Figure 4A)** suggesting an “asthma-like” condition. At high concentrations, SM affected air/blood barrier integrity, resulting in respiratory acidosis, which began at 24 hrs and continued to approximately 60 days PE. This has been described in other animal SM inhalation exposure models (Jugg *et al*., 2013; Veress *et al*., 2015), although over shorter timeframes.

Respiratory dynamics data over the first 24 hrs showed a solid dose-dependent response to SM inhalation with regards to EPAU **(Figures 10A-C),** PEF **(Figures 8A-C),** and peak inspiration flow (**PIF: data not shown**), which is reflected in the MV (**Figures 9A-C**). At 24 hrs PE, SM expired air flow rates did not change, which would indicate that these animals are moving more air than ethanol/saline controls by breathing deeper. EPAU, a pseudo-estimate of lung resistance, shows a marked increase of 1.8-fold vs time-matched ethanol/saline controls at 24 hrs for the

highest-exposure group versus animals. This suggests that airway resistance was limiting the rate of air movement and could explain why the respiratory rates (data not shown) were not consistently increased. This was confirmed by observing MV (respiration rate x tidal volume), which increases in each dose by 10-20% at 24 hrs compared to the respective time-matched ethanol/saline controls. It appears that these animals were expending a great deal of energy respiring, which could explain the high number of animal deaths in the day or two following exposure **(Table 1).** Furthermore, we observed that the PEF rate **(Figure 8A)** was increased more than PIF (data not shown), suggesting that air is easier to move out than in, which is consistent with pseudo-membrane formation in this timeframe **(Figure 23)** yet inconsistent with COPD, where PEF is generally lower.

From weeks 1-11 important changes were seen in the 2.25 and 3.0 mg/kg SM-exposed animals. EPAU showed that airway resistance increased in the two highest SM concentrations. In the 3.0 mg/kg group, this began in the second week, increased through the seventh week, and then began a steady decline. These data suggest an eventual recovery, although this may be obscured somewhat, since similar to the weight gain data, respiratory dynamics improved overall as the sickest animals were culled from the study and thereby are not represented in later data sets. A dose-dependent relationship was apparent in most of the respiratory dynamics results; however, the highest exposure group displayed the greatest effect overall and by far the highest deviation from controls at three weeks, which coincided well with weight loss **(Figure 2)** and mortality rates **(Figure 3, Table 1)** in both high-dosed groups. Examining Te **(Figure 7B),** PEF **(Figure 8B)**, and MV **(Figure 9B)**, it is apparent that these animals were moving much more air via deeper breaths and a faster rate than controls, despite an apparently higher lung resistance (EPAU). This would indicate that the three- to seven-week timeframe represented the greatest respiratory challenge in the 2.25 and 3.0 mg/kg-exposed groups, and aligns well with weight loss and death data during this period. Regarding Te, which is considered to be a bedside indication of COPD**,** there was a decrease (faster time) from 1-11 weeks in the 3.0 mg/kg-exposed group and a delayed general dose-response effect between 13 and 24 weeks **(Figures 7B and 7C, respectively).** It is interesting to note that early in the study the 1.75 and 2.25 mg/kg-dosed groups showed no indication of slower Te (approximating ethanol/saline control levels); however, they ultimately developed a faster rate months PE, signifying that the delayed effects of SM would not have been observed had the study terminated earlier.

Over the period of 11 to 26 weeks, EPAU **(Figure 10C)** increased in the 3.0 mg/kg group through the 15- to 18-week period and then resolved afterward. Similar patterns were seen in PEF **(Figure 8C)** and Te **(Figure 7C).** All of these simultaneous phenomena combined indicate that the 15- to 18-week window represents a persistent and enduring physical challenge to the 2.25 and 3.0 mg/kg groups. Note further that this coincided very well with a third, but far smaller round of animal deaths in the 3.0 mg/kg group **(Figure 3).** Of particular interest are weeks 21 to 26, where decreasing EPAU resulted in an increase in respiratory rate, although MV (the product of respiration rate and tidal volume) was higher than ethanol/saline controls, Te was lower, but peak flows approached normal, thus indicating some modest compensatory measures among the SM-exposed rats. We show that EPAU remained elevated by about 50% at 26 weeks, and 3.0 mg/kg animals seemed to compensate increasing resistance by reducing the pauses between inhalation and exhalation and by inhaling more quickly. Ultimately, respiratory rate and minute volume resolve to nearly control levels. Deaths in this late time-frame were sporadic.

Our data appear to be in conflict with published reports that show a decrease in PEF following exposure to SO_2 in rats, but a negative correlation with goblet cell hyperplasia and the presence of mucous plugs in the respiratory bronchioles (Xu *et al.*, 2000). We measured increases in PEF over time **(Figure 8B)** and in pathology scores for bronchiolar goblet cell hyperplasia, tracheal epithelial necrosis, and perivascular edema starting at about 2 weeks PE in the 3.0 mg/kg SM-exposed rats **(Figure 32A-C).** It is clear that the rat lung response to inhaled SM may fall in a range of compromising conditions that could be inconsistent with those observed in humans.

Morphologically, changes began at about 7.5 hrs PE in the highest SM-exposed group **(Figure 22).** SM triggered the formation of fibrinous pseudo-membranes as early as 24 hrs **(Figure 23),** as well as proteinaceous edema and inflammation by 48 hrs PE **(Figure 25).** Generally, inflammation, fluid-filled alveoli lesions, and mucus plugging of small airways was typical sequelae in SM 2.25 or 3.0 mg/kg-exposed animals in the 3-7 weeks PE timeframe. These are believed to be the cause of the increased airway resistance and poor gas exchange mentioned earlier, thus requiring dramatically greater compensatory ventilation. In support of an asthma-like COPD, **Figures 26, 27, 29, and 30** describe the presence of sub-epithelial proliferation, fibroblast-like cells, and alveolar interstitial fibrosis occurring approximately 31 days to 4 months in the two highest SM- exposed groups. Increased sub-epithelial fibrosis is a marker of airway remodeling that occurs over a range of asthmatic conditions and can be responsible for increased thickening of gas exchange surfaces resulting from COPD (Epstein and Singh, 2001)**.** Asthmatic airway fibroblasts can initiate fibrosis via a higher ratio of tissue inhibitor of metalloproteinase (TIMP-2) to metalloproteinase (MMP-2) (Bergeron *et al.*, 2010). The assessment of an asthma-like condition in the present rat study agrees with that seen in human SM exposures (Balali-Mood and Hefazi, 2006; Pechura and Rall, 1993). Balali-Mood and Hefazi (2006) showed that in 197 SM-poisoned soldiers 78% of the delayed toxic effects were respiratory in nature. Hefazi *et al.* (2005) suggested that 16-20 years after exposure the main complications were COPD, 35%; bronchiectasis, 32.5%; asthma, 25%; and fibrosis, 7.5%. There were even several cases of a restrictive lung disease. Moreover, Emad and Rezaian (1999) showed that in soldiers who survived an acute heavy exposure, the predominating injury was defined by neutrophilic alveolitis. In this study we did see a marked increase in EPAU **(Figures 10A-C).** This pseudomarker of airway restriction was possibly driven by the temporally increased presence of polyps/casts in the airways. Aligned with these pathological states was the presence of inflammation intensified by the presence of neutrophils, eosinophils, and macrophage cells, thereby augmenting the production of reactive oxygen intermediates (ROIs). SM caused enhanced BALF activities of both GPx **(Figure 13)** and CAT **(Figure 15),** suggesting that the presence of neutrophils/monocytes and a hydrogen peroxide-driven free radical environment, which was evidenced by the marked increases in MPO activity **(Figure 16).** This is supported to some extent by the elevated levels of GSH **(Figure 14)** in the BALF. Although we do not have GSH data earlier than 6 weeks, there is clearly strong evidence of an active GSH redox cycle scavenging SM-generated free radicals, which have been shown to be produced by SM (Brimfield *et al.*, 2012). In agreement with the secondary effects of the formation of ROIs is the release of cytokine/chemokine mediators **(Figures 17-20).** While there are few identifiable dose-response effects, there was a clear temporal response. Both BALF IL-1α and IL-1β showed early time profiles PE, most notably within the first two weeks for the two higher SM exposure concentrations **(Figures 17, 18).** The early presence of macrophages, neutrophils, and epithelial cells in the BALF possibly indicates their counteraction against the local toxic effects of SM. BALF GRO/KC (**Figure 19),** a CXCL-1 chemokine**,** showed a variable temporal response across

all three SM exposure concentrations compared to time-matched ethanol/saline controls. GRO/KC is a chemoattractant for neutrophils, which were shown in the histopathology through the course of injury, and is confirmation of locally concentrated neutrophil activity. Lavage IL-7 **(Figure 20)** is also a product of SM toxicity in the lung milieu. IL-7 not only plays a role in T-/B- cell development, but is released from the bone marrow and produced by epithelial and dendritic cells, both of which are present in the lung. We measured the temporal effects of SM exposure across each exposure concentration on RBC and WBC shape, size, and volume in the bone marrow isolated from rat femurs. The data (not shown) were inconclusive except for the RBCs, which had smaller diameters at later time points and for the highest SM exposure concentration compared with ethanol/saline controls. **Table 2** shows the temporal aggregate expression fold changes of selected BALF cytokines/chemokines. Although none showed any specific time point-related dose-response effects, several demonstrated marked differences when considering the 6-month total temporal output versus ethanol/saline controls. For instance, the chemokine MIP-1α (CCL3), IL-5 and IL-6 showed a clear dose-related response effect. MIP-1α is produced by macrophages. It is a chemoattractant for neutrophils, resulting in neutrophilic inflammation, which was shown at about 48 hrs PE in the two highest SM-exposed groups **(Figure 25).** In addition, it is critical for immune responses because it acts as a chemoattractant for T-/B-cells (Mauer *et al.*, 2004). B-cells have been shown to be important in the pathogenesis of certain COPD conditions such as emphysema (Polverino *et al*., 2016). IL-5, which is a byproduct of T-helper-2 cells and a marker of asthma, showed a dose-dependent temporal increase over ethanol/saline controls along with the pro-inflammatory cytokine and immune function regulator IL-6. Upregulation of both IL-5 and IL-6 has been shown to be important in the progression and severity of asthma (Bradding *et al*. 1994; Peters *et al.*, 2016). In our model, the marked dose-dependent aggregate temporally increased expression of IL-5 and IL-6 supports the respiratory dynamic and histopathology data suggesting a condition of asthma in the survivors. Bradding *et al.* (1994) demonstrated that mast cells are pivotal in the progression of asthma, most importantly with regard to the production of TNFα. Although the presence of mast cells was not determined in this study, the fold-increase expression of TNFα for each exposure concentration may point to mast cell contribution as the injury progresses**.** This diagnosis is further supported by the fold increase in IL-17 and the decrease in IL-12, both of which are reported to be heavily involved in asthma etiology. IL-17 is associated with allergic responses, is an indicator of tissue remodeling, and is involved in chronic inflammation as well as immune regulatory processes. It is also a key mediator of COPD, contributing to lesion formation (Polverino *et al*., 2016). Kawaguchi *et al.* (2009) reported that a member of the IL-17 family, IL-17F, plays a significant role in asthma**.** In relationship to the presence of IL-17 and inhaled SM-induced lung injury, at 30 days PE an accumulation of IL-17 was demonstrated in inflamed monkey lungs (Mishra *et al*., 2012). There is a link between the presence of IL-17 with COPD, particularly in asthma (Shen *et al*., 2004). In the current study our assay for IL-17 could not distinguish between separate family members. Bergeron *et al.* (2010) suggest that up-regulation of IL-12 levels may aid in ameliorating asthma. Both IL-4 and IL-13 are also important in the asthma (Bergeron *et al.* 2010); however, while they were both measured in this study, they did not differ from ethanol/saline controls. With respect to the lung, we are well aware that the mediators discussed are in constant contact with each other pertaining to the sites of production and available substrates. As such, the resulting admixed microenvironment could potentiate an adverse biological outcome. This was demonstrated by Honda *et al.* (2016) regarding the synergistic effects of IL-17A and TNFα on amplification of airway inflammation. Thus, we made

no attempt to discuss the complicated interaction between inflammatory mediators in this lung injury model.

Decreased body weights, increases in mortality, changes in respiratory dynamics, increased activity of ROI pathways, compromised immuno-function and deleterious changes in lung pathology were prevalent within the first five weeks PE. These coupled to alveolar exudates, edema, and inflammation peaking at roughly 3 weeks correlated well with compensatory changes in pulmonary function and/or respiratory distress. Animals that demonstrated respiratory distress at three weeks were more likely to die later in the study. Notably, this indicates that 3-6 weeks PE in this model may be a crucial window in the progression of SM inhalation lung injury, and that therapeutic intervention prior to and concurrent with this time point may offer the best approach as a medical countermeasure. Based on this information, herein we provide preliminary evidence of the effects of a PE mesenchymal stem cell therapeutic approach. An infusion of MSCs 4-6 hrs PE was effective in reducing SM-induced edema, necrosis, inflammation, and death at 3-6 weeks **(Figure 33).** Surprisingly, we also show that saline hydration therapy could be effective as well in reducing the toxicity of SM **(Figures 35A-C).** Work by Kotton and Fine (2003) and Krause *et al.* (2001) demonstrated that bone marrow-derived MSCs can serve as progenitors of Type II lung and bronchial cells. The mechanisms responsible for MSCs in tissue remodeling may involve the up-regulation of a family of Wnt proteins and TGF-β_1, both of which are responsible for fibrosis and the enhancement of tissue remodeling (Salazar *et al*., 2009). While tissue remodeling is critical in the healing process it can affect the lung's capability to inflate and deflate, ultimately resulting in COPD, asthma, and bronchiolitis. In the current study, we were not able to verify through fluorescent imaging the location of the injected MSCs. We do show, however, that MSC therapy reduced both the overall pathology scores as shown in **Figure 34** and scores for bronchiolar goblet cell hyperplasia, epithelial necrosis and tracheal exudates **(Figures 35A-C).** Limited success with MSCs may be treatment interval-dependent. In part this may be why in lung exposure challenge models there is some measure of resolution of acute tissue injury (Gupta *et al.*, 2007; Ortiz *et al.*, 2003; Zhang *et al.*, 2016).

This study provides the first long-term examination of SM-induced lung injury and its systemic effects. It further demonstrates the feasibility of stem cell therapies for treatment of SM inhalation injury as shown by lower mortality rates and pathology scores. We envision the next phase of this work to include multiple challenges with MSCs during the course of injury development since success may be time/frequency treatment-dependent. Aggressive therapeutic use of MSCs early in the injury process may eliminate or at least ameliorate the numerous toxidromes observed in this study. As is evident from the temporal responses among the data herein, we can deduce that therapeutic intervention over time could be a challenge, with difficulties in addressing the variable compromised conditions of respiratory efficiency over different timeframes.

In summary, a critical weakness of the state of research on SM-induced lung injury is the significant absence of data involving the long-term effects and recovery from SM inhalation exposure, especially when considering the long-term outcomes seen in the Iran-Iraq War survivors. Although there is consistent evidence that inhaled SM causes acute lung damage 28-30 days PE, our data demonstrate that there are adverse effects spread over a six-month period following a single initial inhalation challenge. These appear to occur in several key windows (i.e., 3-6 weeks and 12-16 weeks PE in the highest exposure concentration) and are coupled to

unpredictable lethality inflection points within those timeframes. However, the dose-dependent timing and uncertainty of the mechanisms behind the recurrent nature of these adverse events would make them difficult to predict. This is problematic because traditional treatment intervention during the acute phase may not be adequate since survivors show clear signs of other toxidromes over time. Our data align quite well with the Iranian survivor experience years after the Iran-Iraq War. As such and in conjunction with human data, we provide evidence that a single exposure to SM aerosol for 10 minutes produced a range of physiological, toxicological and pathophysiological complications over time that may complicate rational and timely medical intervention. We also show that treatment with stem cells could be a potential medical countermeasure in reducing toxidromes associated with long-term SM inhalation toxicity.

REFERENCES

Aasted A, Wulf, HC, Darre, E, Niebuhr E (1985). Fishermen exposed to mustard gas: clinical experiences and cancer risk evaluation. *Ugeskr Laeger* **147**:2213-2216.

Allon N. Amir A, Manisterski E, Rabinovitz I, *et al.* (2009). Inhalation exposure to sulfur mustard in the guinea pig model: Clinical, biochemical and histopathological characterization of respiratory injuries. *Toxicol Appl Pharmacol* **241**:154-162**.**

Anderson DR, Yourick JJ, Moeller RB, Petrali JP, *et al.* (1996). Pathologic changes in rat lungs following acute sulfur mustard inhalation. *Inhal Toxicol* **8**:285-297.

Atkins KB, Lodhi IJ, Hurley LL, and Hinshaw DB (2000). N-acetylcysteine and endothelial cell injury by sulfur mustard. *J of Appl Toxicol* **20,** S125-S128.

Balali-Mood M, Hefazi, M (2005). The pharmacology, toxicology, and medical treatment of sulphur mustard poisoning. *Fund Clin Pharmacol* **19**:297-315.

Balali-Mood M, Hefazi M. (2006). Comparison of early and late toxic effects of sulfur mustard in Iranians veterans. *Basic & Clin Pharmacol & Toxicol* **99:**273-282.

Bánfi A, Tiszlavicz L, Székely E, Pétak F, et al. (2009). Development of bronchus-associated lymphoid tissue hyperplasia following lipopolysaccharide-induced lung inflammation in rats. *Exp Lung Res* **35**:186-197.

Bergeron C, Tulic MK, Hamid Q. (2010). Airway remodeling in asthma: From benchside to clinical practice. *Can Respir J* **17**(4):e85-e93.

Bradding P, Roberts JA, Britten KM, Montefort S, *et al.* 1994). Interleukin-4, -5, and -6 and tumor necrosis factor-alpha in normal and asthmatic airways: evidence for the human mast cell as a source of these cytokines. *Am J Respir Cell Mol Biol* **10** (5):471–80.

Brimfield AA , Soni, SD , Trimmer, KA, Zottola MA, *et al.* (2012). Metabolic activation of sulfur mustard leads to oxygen free radical formation. *Free Rad Biol and Med* **52**:811-817.

Capacio BR, Smith JR, Lawrence RJ, Boyd BL, *et al.* (2008). Gas chromatographic-mass spectrometric analysis of sulfur mustard-plasma protein adducts: validation and use in a rat inhalation model. *J Anal Toxicol* **32**(1): 37-43.

Casillas RP, Mitcheltree LW, Stemler FW (1997). The mouse ear model of cutaneous sulfur mustard injury. *Toxicol Meth* **7**:381-397.

Dacre JC, Goldman M (1996). Toxicology and pharmacology of the chemical warfare agent sulfur mustard. *Am Soc Pharmacol Exp Ther* **48**:289-326.

Dillman JF III, Phillips, CS, Dorsch LM, Croxton MD, *et al.* (2005). Genomic analysis of rodent pulmonary tissue following bis-(2-chloroethyl) sulfide exposure. *Chem Res Toxicol* **18**:28-34.

Eisenmenger W, Drasch G, von Clarmann M, Kretschmer E., *et al* (1991). Clinical and morphological findings on mustard gas [bis(2-chloroethyl)sulfide] poisoning. *J Forensic Sci* **36**(6):1688-98.

Emad A, Rezaian GR. (1999). Immunoglobulins and cellular constituents of the BAL fluid of patients with sulfur mustard gas-induced pulmonary fibrosis. *Chest* **115**(5):1346-1351.

Epstein SK, Singh N. (2001). Respiratory acidosis. *Respir Care* **46**(4):366-383.

Fairhall SJ, Jugg, BJA, Read RW, Stubbs SJ, *et al*. (2010). Exposure-response effects of inhaled sulfur mustard in a large porcine model: a 6-h study. *Inhal Toxicol* **22**:1135-1143.

Ghanei M, and Harandi AA (2007). Long term consequences from exposure to sulfur mustard: a review. *Inhal Toxicol* **19**:451-456.

Gold MB, and Scharf BA (1995). Hematological profile of the euthymic hairless guinea pig following sulfur mustard vesicant exposure. *J of Appl Toxicol* **15(6):**433-438.

Gopinath CC and Mowat V (2014). The Respiratory System. In: *Atlas of Toxicological Pathology.* Chapter 2, Eds Gopinath C C, Mowat V, Springer, New York, pp 19-45-4.

Gupta N, Su X, Popov B, Lee JW, *et al.* (2007). Intrapulmonary delivery of bone marrow-derived mesenchymal stem cells improves survival and attenuates endotoxin-induced acute lung injury in mice. J Immunol **179**:1855-1863.

Hefazi M, Attaran D, Mahmoudi M, Balali-Mood M. (2005). Late respiratory complications of mustard gas poisoning in Iranian veteran. *Inhal Toxicol* **17**:587-592.

Honda K, Wada H, Nakamura M, Nakamoto K, *et al.* (2016). IL-17A synergistically stimulates TNFα-induced IL-8 production in human airway epithelial cells: A potential role in amplifying airway inflammation. *Exp Lung Res* (42):**4** 205-216.

Hurst CG, Smith WJ (2008). Health Effects of Exposure to Vesicant Agents. In: *Chemical Warfare Agents – Chemistry, Pharmacology, Toxicology, and Therapeutics.* Eds, Romano JA, Lukey BJ, Salem, H, 2nd ed., CRC Press, Boca Raton, FL. pp 294-312.

Jugg B, Fairhall S, Smith S, Rutter S, *et al.* (2013). N-acetyl-L-cysteine (NAC) protects against inhaled sulfur mustard (HD) poisoning in the large swine. *Clin Toxicol* **51**:216-224.

Kan RK, Tompkins CM, Kniffin DM, Hamilton TA, *et al.* (2008). Lung pathology induced by sulfur mustard and the nerve agent soman. Medical Defense Bioscience Review, U.S. Army Medical Research Institute of Chemical Defense. June, p 177.

Kawaguchi M, Kokubu F, Fujita J, Huang SK, Hizawa N (Dec 2009). Role of interleukin-17F in asthma. *Inflammation & Allergy Drug Targets* **8** (5): 383–9.

Kehe, K and Szinicz L. (2005). Medical aspects of sulphur mustard. *Toxicol* **214**:198-204.

Korkmaz A, Yaren H, Topal T, and Oter S. (2006). Molecular targets against sulfur mustard toxicity: implication of cell surface receptors, peroxynitrite production and PARP activation. *Arch Toxicol* **80**:662-670.

Kotton DN and Fine A (2003). Derivation of lung epithelium cells from bone marrow cells. *Cytotherapy* **5**(2):169-173.

Krause DS, Theise ND, Collector MI. (2001). Multiorgan, multi-lineage engraftment by a single bone marrow-derived stem cell. *Cell*, **105**:369-77.

Kumar O, Sugendran K, and Vijayaraghavan, R. (2001). Protective effect of various antioxidants on the toxicity of sulphur mustard administered to mice by inhalation or percutaneous routes. *Chem-Biol Interact* **134**:1-12.

Laskin JD, Black AT, Jan Y-H, Sinko PJ, *et al.* (2010). Oxidants and antioxidants in sulfur mustard-induced injury. *Ann NY Acad Sci* **1203**:92-100.

Lowry OH, Rosebrough NJ, Farr AL, *et al*. (1951). Protein measurement with Floin phenol reagent. J Biol Chem **193**:265-275.

Malaviya, R, Sunil, VR, Cervelli, J, Anderson, DR, *et al*. (2010). Inflammatory effects of inhaled sulfur mustard in the rat lung. *Toxicol Appl Pharmacol* **248**:89-99.

Maurer M, von Stebut E (2004). Macrophage inflammatory protein-1. Int. J. Biochem. Cell Biol. **36** (10):1882–6.

Meier H L, Clayson ET, Kelly SA, Corun CM (1996). Effect of sulfur mustard (HD) on ATP levels of human lymphocytes cultured *in vitro*. *In Vitro Toxicol* **9(2):**135-139.

Mishra, NC, Rir-sima-ah, J, Grotensdorst, GR, Langely, RJ, *et al.* (2012). Inhalation of sulfur mustard causes long-term T cell-dependent inflammation: Possible role of Th17 cells in chronic lung pathology. *Int Immunopharmacol* **13**(1):101-108.

Nishimura, Y, Iwamoto, H, Ishikawa, N, Hattori, N, *et al.* (2016). Long-term pulmonary complications of chemical weapons exposure in former gas factory workers. *Inhal Toxicol* **28:**343-348.

Ortiz LA, Gambelli F, McBride C, Gaupp D, *et al*. (2003). Mesenchymal stem cell engraftment in lung is enhanced in response to bleomycin exposure and ameliorates its fibrotic effect. *Proc Nat Acad Sci* **100**(14):8407-8411.

Otto GM, Franklin CL, Clifford CB. (2015). Biology and diseases of rats. In: *Laboratory Animal Medicine*. Eds. Fox JG, Anderson LC, Otto, G, Pritchett-Corning KR, and Whary MT. Academic Press, London, pp 151-207.

Pechura CM, and Rall DP (1993). Relationship of mustard agent and lewisite exposure. In: *Veterans at Risk, the Health Effects of Mustard and Lewisite*. National Academy Press, Washington, DC USA, pp: 81-111.

Peters MC, McGrath KW, Hawkins GA, Hastie AT, *et al.*, (July 2016). Plasma interleukin-6 concentrations, metabolic dysfunction, and asthma severity: a cross-sectional analysis of two cohorts. *The Lancet Resp Med* **4** (7): 574–84.

Pohl C, Papritz M, Moisch M, Wübbeke C, *et al*. (2009). Acute morphological and toxicological effects in a human bronchial co-culture exposure model after sulfur mustard exposure. *Toxicol Sci* **112**(2):482-489.

Polverino F, Seys LJM, Bracke KR, Owen CA. (2016). B cells in chronic obstructive pulmonary disease. *Am J Physiol Lung Cell Mol Physiol* **311**:L687-L695.

Rao PVL, Vijayaraghavan R, Bhaskar ASB (1999). Sulphur mustard induced DNA damage in mice after dermal and inhalation exposure. *Toxicol* **139**:39-51.

Ray R, Keyser B, Benton B, Daher A, *et al*. (2008). Sulfur mustard induces apoptosis in cultured normal human airway epithelial cells: Evidence of a dominant caspase-8-mediated pathway and differential cellular response. *Drug and Chem Toxicol* **31**:137-148.

Salazar KD, Lankford SM, Brody AR. (2009). Mesenchymal stem cells produce Wnt isoforms and TGF-β_1 that mediate proliferation and procollagen expression by lung fibroblasts. *Am J Physiol Lung Cell Mol Physio,* **297**:L1002-L1011.

Sawyer TW (1999). Toxicity of sulfur mustard in primary neuron culture. *Toxicol In Vitro* **13**: 249-258.

Sciuto AM., Moran, TS, Forster, JS, and Cascio, MB (2000). Intravenous sulfur mustard (HD) increases the production of cytokines in the bronchoalveolar lavage fluid (BALF) from rats. Bioscience Proceedings, CBRNIAC-CB, Accession Number 177978.

Sciuto AM, Moran TS, Phillips C, Dillman JF III (2007). Induction of lung injury in rats following a non-traditional exposure to sulfur mustard. Poster Presentation: International Union of Toxicology (IUTOX), Montreal, Quebec, Canada, July, PT1.012.

Shen F, Zhao MW, He B, Yang JJ, *et al*. (2004). The changes and significance of interleukin-17 in rat models of chronic obstructive pulmonary disease and asthma. *Zhonghua Jie He He Hu Xi Za Zhi* **10**:654-658.

van Helden HPM, Kuijper WC, Diemel RV (2004). Asthma-like symptoms following intratracheal exposure of guinea pigs to sulfur mustard aerosol: Therapeutic efficacy of exogenous lung surfactant curosurf and salbutamol. *Inhal Toxicol* **16**: 537-548.

Veress LA, Anderson DR, Hendry-Hofer TB, Houin PR (2015). Airway tissue plasminogen activator prevents acute mortality due to lethal sulfur mustard inhalation. *Toxicol Sci* **143**(1): 178-184.

Vijayaraghavan R, Sugendran K, Pant SC, Husain K, *et al*. (1991). Dermal intoxication of mice with bis(2-chloroethyl)sulphide and the protective effect of flavonoids. *Toxicol* **69**:35-42.

Vijayaraghavan R. (1997). Modifications of breathing pattern induced by inhaled sulphur mustard in mice. *Arch Toxicol* **71**:157-164.

Wheeler GP (1962). Studies related to the mechanisms of action of cytotoxic alkylating agents: a review. *Cancer Res* **22**:651-688.

Willems JL (1989). Clinical management of mustard gas casualties. *Annales Medicinae Militaris (Belgicae*), Vol 3/supplement, 1-61.

Wulf HC, Aasted A, Darre E, Niebuhr E (1985). Sister chromatid exchanges in fishermen exposed to leaking mustard gas shells. *Lancet* **1**:690-691.

Xu J, Zhao M, Liao S. (2000). Establishment and pathological study of models of chronic obstructive pulmonary disease by SO_2 inhalation model. *Chin Med J* **113**(3): 213-216.

Zhang J, Shao Y, He D, Zhang L, *et al.* (2016). Evidence that bone marrow-derived mesenchymal stem cells reduce permeability following phosgene-induced acute lung injury via activation of wnt3a protein-induced canonical wnt/β-catenin signaling. *Inhal Toxicol* **28**(12): 572-579.